Microfabrication Using Shape-Transforming Soft Materials

Indra Apsite, Arpan Biswas, Yuqi Li, and Leonid Ionov*

The fabrication of hollow and multicomponent micro-objects with complex inner structures using state-of-the-art subtractive, formative, and additive manufacturing technologies is challenging. Controlled shape transformation offers a very elegant solution to this challenge. While shape transformations on macroscale can be achieved using either manual or automatic manipulation, shape transformations on microscale can better be realized using shape-changing polymers such as hydrogels, shape-memory polymers, liquid crystalline elastomers, and others. This review discusses the properties of different classes of shape-changing materials, the principle of shape transformation, possibilities to achieve complex shape transformation, as well as applications of shape-changing materials in microfabrication and other fields.

1. Introduction

The development of methods for fabrication is important for every aspect of our life: from building of houses, assembling of cars to microelectronic devices. There is broad pallet of methods for fabrication of macroscopic object including subtractive manufacturing (lathe, cutting, milling), additive manufacturing (3D printing), and formative manufacturing (molding). Some of these methods are computerized that allows programmable fabrication of very complex parts. While most of these methods provide acceptable quality at a reasonable price of macroscopic objects, attempts to downscale them and to increase resolution results in a tremendous increase in costs. In particular, the milling machine (subtractive manufacturing) is efficient for the fabrication of centimeter larger objects, and the size of the drill determines the resolution. Fabrication of millimeter and sub-millimeter objects requires very fine drills and very expensive

I. Apsite, Dr. A. Biswas, Dr. Y. Li, Prof. L. Ionov
Faculty of Engineering Science
Department of Biofabrication
University of Bayreuth
Ludwig Thoma Str. 36A, 95447 Bayreuth, Germany
E-mail: Leonid.Ionov@uni-bayreuth.de
Dr. Y. Li
College of Materials Science and Engineering
Guilin University of Technology
Jiangan Str. 12, 541004 Guilin, China
Prof. L. Ionov
Bavarian Polymer Institute
Universitätsstr. 30, 95440 Bayreuth, Germany

The ORCID identification number(s) for the author(s) of this article can be found under https://doi.org/10.1002/adfm.201908028.

machines to control them. The same can be applied for 3D printing. Different 3D printing methods like fused deposition modeling (FDM; extrude thermoplastic filaments above its melts temperature) and laser sintering are very successful for the fabrication of centimeter-large objects; they fail when are used for fabrication of the submillimeter and microsized object.[1,2] Stereolithography allows 10 µm resolution but is limited for the use of certain materials and has difficulties with the fabrication of hollow objects. Two-photon polymerization allows unprecedented resolution, but it is limited for very specific substances and is very expensive and slow.[3] Molding may be considered as the cheapest technology for fabrication of small elements if one does not consider that molds have to be fabricated firsthand by some other techniques. Fabrication of hollow objects and multicomponent objects with complex inner structure is even more challenging.

One possibility for the fabrication of complex shapes is the use of controlled shape transformation. The most brilliant example of the applicability of controlled shape transformation for the fabrication of complex shapes is the Japanese art of paper folding—Origami. While folding of macroscopic objects can be done either manually or by using special machines, folding of micro-objects is not trivial—the machines, which allow micromanipulation, are expensive and allow low throughput. One suitable solution is to use special materials, which are capable of controlled shape transformation. All these materials possess different mechanical and actuation properties that make them more suitable for some and less suitable for other applications (**Table 1**). This review discusses basic principles of design of such materials, their mechanical and actuation properties, principles of complex shape transformation, and application of shape transformation in the field of microfabrication and others.

2. Shape Changing Materials

Shape changing polymers are smart polymeric materials that are capable of changing their shapes in the presence of certain external stimuli.[4] All shape-changing polymers have several features, which allow their reversible shape-transformation. First, they must be able to demonstrate elastic deformation that is commonly provided by the presence of crosslinking points. Namely, crosslinking points are responsible for the reversibility of deformation. These crosslinking points can be either covalent or physical bonds such as crystallites, glassy-hard domains, H-bond, ionic interactions, etc. and molecular switches, which are sensitive external stimuli. Based on these, some polymeric

**ADVANCED
SCIENCE NEWS**
www.advancedsciencenews.com

**ADVANCED
FUNCTIONAL
MATERIALS**
www.afm-journal.de

building blocks have been recognized which are appropriate for demonstrating shape-changing behavior (**Figure 1**). Covalently connected polymer frameworks are the most common example of shape-changing polymers in which switching segments are connected via covalent bonds and produce net points (Netpoint is typically the connection point of the polymer chains which helps in determining the permanent shape of shape-changing polymers) (Figure 1a). In some shape-changing polymers, the covalently connected frameworks have some side chains attached to the main chain, which can form a segregated phase, as observed in (Figure 1b). Sometimes the reversible bonding between two side chains also helps in showing shape-changing behavior (Figure 1c). The triblock copolymers with multiphase morphologies (Figure 1d) or some copolymers with liquid crystal elastomer as a switching segment also belong to this class (Figure 1e). Furthermore, the physical interactions like dipole–dipole interactions, hydrogen bonding or ion rich domains are also capable of producing net point for showing shape-changing behavior (Figure 1f).[5,6] Apart from these molecular architectures, sometimes processing and capillary phenomenon also plays some role in producing shape-changing behavior in polymers. Elastic deformation is also observed for semicrystalline and glassy polymers at low deformation degree.

Second, polymer chains must be in the state when they are mobile or undergo a transition between mobile and immobile states. Thus, polymers can demonstrate shape-changing properties either above their glass transition/melting point or at a temperature close to it. Third, shape-changing polymers must be sensitive to stimuli that are provided by the presence of certain chemical groups or additives, which are sensitive to pH, ionic strength, light, electromagnetic field, magnetic field, etc.[7] Meanwhile, all polymers demonstrate sensitivity to temperature when the temperature is varied around glass transition/melting. In this part of the review, the principles or mechanisms which are responsible for triggering the shape-changing behaviors in different classes of polymers will be discussed thoroughly.

2.1. Relaxation Phenomena (Shape-Memory Polymer)

Shape memory behavior is an entropic phenomenon, and it is associated with the relaxation behavior of the polymer chains or segments.[8,9] Many mechanisms have been proposed to describe the shape memory behavior of polymers considering the relaxation behavior of polymeric segments. Typically, shape memory polymers (SMPs) consist of switching segments that are capable of reversible phase transformation at a transition temperature (glass transition or melting temperature transition) and shape determining segments or net points that prevent the permanent deformation.[10–12] In initial shape, the polymer chains remain in a coiled state which is the low energy state (highest entropy), and any macroscopic deformation above the transition temperature (glass or melting) keeping the network structure intact would cause conformational changes of polymer chains along with enhancement in the energy state (**Figure 2**a).[8] The freezing of that conformation below the transition temperature allows the system to maintain its high energy state. Further, heating above transition temperature helps the molecular chains to recover their permanent configuration utilizing the entropic energy.

Indra Apsite received her Bachelor's and Master's degree in chemistry from the University of Latvia (Riga) in 2013 and 2015, respectively. She is currently a Ph.D. candidate at University of Bayreuth (Germany) under the supervision of Prof. Leonid Ionov, and her current research focuses on fibrous shape-morphing materials as a substrate for biofabrication and tissue engineering of skeletal muscle and nerve tissues.

Arpan Biswas is currently working as a research associate at the Faculty of Engineering Science, Biofabrication, University of Bayreuth. He received his Ph.D. from IIT (BHU) in 2018 and completed his M.Sc. from West Bengal State University, West Bengal. His research interests include designing and 3D printing of smart stimuli-responsive polymers for biomedical applications.

Leonid Ionov is a professor for biofabrication at the University of Bayreuth. He graduated in chemistry in 1999 from Lomonosov Moscow State University and completed his Ph.D. in 2005 as well as habilitation in 2015 at Dresden University of Technology. After that he worked at the University of Georgia as a faculty member. His main research activities are focused on 3D printing and bioprinting as well as on shape-changing polymers.

So, the storage and release of entropic energy through conformational changes is the driving force for executing the shape memory behavior in polymers. The relaxation behavior or viscoelastic property of the molecular chains of SMPs also contributes to the molecular mechanism of shape memory behavior. Hence, the thermoviscoelastic model is perfect to describe the shape-memory phenomena in polymers. Initially, different thermoviscoelastic models have been proposed considering stress relaxation as a simple phenomenon,[13–15] and it is very easy to describe such simple relaxation behavior only by one Maxwell or Kelvin–Voigt element. However, in a real case, the

**ADVANCED
SCIENCE NEWS**

www.advancedsciencenews.com

**ADVANCED
FUNCTIONAL
MATERIALS**

www.afm-journal.de

Table 1. Mechanical and actuation properties of various shape-changing materials.

Materials	Young's modulus [MPa]	Tensile/actuation stress [MPA]	Elongation at break/actuation strain [%]	Actuation time	Recovery ratio [%]	Lifting weights [times]	Work density [j g⁻¹]	Ref.
Hydrogels	0.008–5.6	0.01–8.3	150–1500	10–600 s	90–99	25–60	N/A	[61–68]
Shape memory polymer	0.82–349	8.9–24.3	130–1240	10–1500 s	81–99.3	600–3500	N/A	[69–75]
Dielectric elastomer	0.03–5	0.1–4	4.5–215	1.0 ms–1.0 s	N/A	1.0–16.7	0.03–0.15	[25,76–80]
Liquid crystal elastomers	2.0–177.8	0.038–25	120–475	1.0–1200 s	85–99	250–5680	N/A	[81–86]

relaxation phenomenon is very complex for polymers because of their complicated structure, and it requires multiple parameters to describe. For example, Mulliken and Boyce proposed a model considering two Maxwell branches to describe α and β

Figure 1. Examples of some typical molecular architecture which are suitable for showing shape-changing behavior: a) The covalent bonds between the switching segments (red color) produces net points (gray color); b) the side chain acts as switching segment in this case; c) the reversible bonding between the functional group (red color) acts as molecular switches; d) ABA triblock system acts as the switching segments and produces the net point at junction; e) the organized mesogens in liquid crystal elastomers acts as the switching domains; f) the physical interaction like dipole–dipole interactions, H-bonding, etc. produces the net point. Reproduced with permission.[5,6] Copyright 2013, Royal Society of Chemistry.

transitions in polymers due to different strain rates.[16] Further, Zhao et al. reported that the isothermal crystallization behavior with the time of a polymeric network is the responsible factor for triple/multiple shape-memory behaviors in polymers.[17] The isothermal crystallization generally consists of primary and secondary crystallization. In primary crystallization, the crystals are formed through nucleation of the amorphous chains of the polymers without any intervention on the confinement of the crystals while the secondary crystals grow in the part of the amorphous regions which are already interfaced by the primary crystals.(Figure 2b) Usually, the secondary crystals are thinner (low melting temperature) as compared to primary crystals (high melting temperature), and when this thickness difference becomes significant, it produces distinct melting endotherms. These multiple melting endotherms help the polymer to show triple or multiple shape-memory effect.[18] The energy released during the melting of the crystals helps the polymeric materials to regain its permanent shape. Behl et al. reported temperature-sensitive polymer actuation considering the broad melting temperature range of a semicrystalline polymer network.[19] According to them, crystallites with different melting temperatures act as bricks as well as temperature-responsive volume changing units. The crystallites with a lower melting temperature are responsible for reversible actuation while the crystallites with a high melting temperature act as a skeleton forming domains. (Figure 2c) The macroscopic shape actuation of semicrystalline polymers is only possible if the domains are aligned in the matrix and are connected covalently. A "spring model" is proposed by Biswas et al., considering the molecular flipping of some crystalline parts to demonstrate the molecular mechanism of reversible bidirectional shape memory behavior.[20] In this model, the soft segments (blue color) of the polymer are sandwiched between hard segments (red color) and some hard segments are also distributed within the soft segment part in the presence of strong interaction. (Figure 2d) Now, above the transition temperature, the distributed hard segment starts to move toward the consolidated hard segments along with the coiling of the liquid soft segment that again redistributed within the soft segments during cooling. Thus, reversible flipping of the tiny hard segments with heating–cooling cycles at the molecular level helps to trigger reversible shape memory behavior in polymers macroscopic levels.
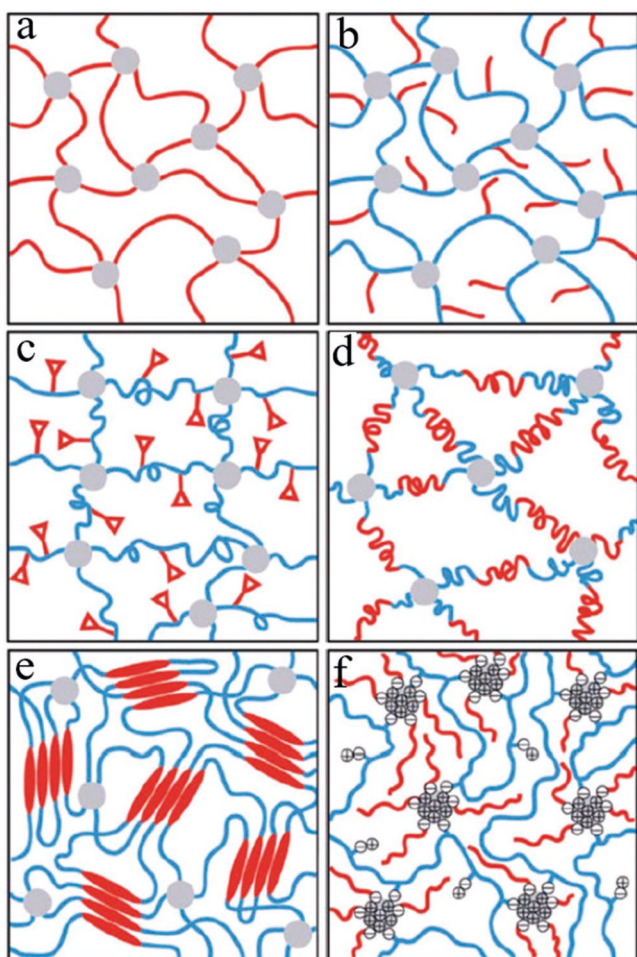
2.2. Dielectric Elastomer

Dielectric elastomers are another kind of shape-changing polymers, whose actuation is based on relaxation. Dielectric

ADVANCED
SCIENCE NEWS
www.advancedsciencenews.com
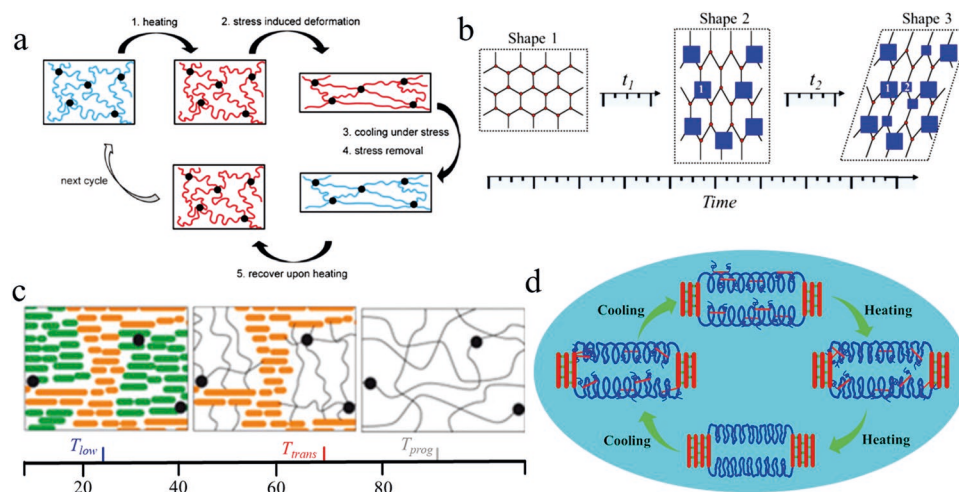
ADVANCED
FUNCTIONAL
MATERIALS
www.afm-journal.de

Figure 2. Relaxation as a driving force in shape memory behavior: a) the molecular mechanism of shape memory behavior in a chemically crosslink polymer moiety. The stored energy in the molecular backbone after fixing the deformed shape through cooling provides sufficient energy during the recovery process, Reproduced with permission.[8] Copyright 2015, Elsevier; b) time depended crystallization in the amorphous part of the polymer chain responsible for the triple shape memory behavior, Reproduced with permission.[17] Copyright 2015, Elsevier; c) in this model, the crystallites are like bricks and reversible melting and crystallization of some bricks with a low melting temperature with temperature cycles triggering reversible shape memory actuation, Reproduced with permission.[19] Copyright 2013, United State National Academy of Science; d) in this spring model, reversible flipping of some tiny crystallites along with the actuation domain triggering the reversible shape-changing behavior. Adapted with permission.[20] Copyright 2016, American Chemical Society.

elastomers are placed between two compliant electrodes and acts as a compliant capacitor model. The application of voltage to the electrodes placed on the opposite side of the elastomer creates opposite net charges, which form stress (Maxwell stress) in the elastomeric film due to electrostatic attraction (coulombic attraction). This so-called Maxwell stress triggers the thinning of the dielectric elastomer which is further compensated by the expansion in the plane of elastomer (**Figure 3**a). This expansion strain is sufficient enough to activate the shape-changing behavior in the dielectric elastomer.[21] However, the uniform electric field throughout elastomer restricts the switching of the elastomer to a new shape, but the presence of a passive layer can introduce the bending actuation in the material. According to the compliant capacitor model, the actuators can show either in-plane expansion,[21] liner actuation,[22,23] or bending.[24] The stress and strain produced by the parallel plate actuation are equal in both perpendicular direction ($\sigma_x = \sigma_y = -1/2\sigma_z$),[25] which is not desired all the time, and to overcome this limitation different strategies have been considered. For example, the attachment of a passive layer with the flexible dielectric elastomer and the electrode on both sides helps in converting the voltage induced linear expansion into a flexural actuation.[24] Figure 3b shows different bending behavior of the bilayer structure consisting of a dielectric elastomer (active layer) and fibers (passive layer), with varying fiber configuration. In an another approach, Hajiesmaili and Clarke demonstrated that the shape morphing of dielectric elastomers can be manipulated by varying the spatial distribution of the electric field using an internal mesoarchitecture of the electrodes.[26] The actuation of a strip into a torus structure with positive curvature (outer part of the torus) or negative curvature (inner part of the torus) can be achieved by changing the width of the electrode gradually from bottom to top, as observed in Figure 3c. The strip with decreasing electrode's width from bottom to top (11 to 1 mm) results in torus structure with

positive curvature while strip with increasing electrode's width results in torus structure with negative curvature.

2.3. Volume Change (Swelling Hydrogels)

Shape changing hydrogels are water-swollen crosslinked frameworks, which are capable of reversible swelling/deswelling with changes in environmental water contact due to change of affinity of polymer chains toward the water.[27,28] The degree of swelling of any hydrogels is directly associated with crosslinking density and molar free energy of mixing which is again the function of interchain interactions, solvents, and entropy of mixing (Flory–Rehner Theory). So, if the average molar mass of the connecting moieties between two adjacent network nodes is $\overline{M_c}$, the crosslinking density (ν_c) of the crosslinked polymeric network can be calculated using the Flory–Rehner equation (Equation (1))[6]

$$\nu_c = \frac{\ln(1-\varphi_2)+\varphi_2+\varphi_2^2\chi_{12}}{V_1\left[\left(\frac{\varphi_2}{2}\right)-\varphi_2^{1/3}\right]} = \frac{\rho}{\overline{M_c}} \tag{1}$$

where, χ_{12} is responsible for Flory solvent–polymer interaction, ρ is the density of the network, V_1 is the molar volume of the solvent and the φ_2 is the volume fraction of the polymer in the swollen state ($\varphi_2 = V_d/V_{sw}$; V_d is the volume in the dry state, and V_{sw} is the volume in the swollen state).

For hydrogels with a constant crosslinking density, the entropic and energetic components can be influenced by the temperature and solvent quality, which again associated with temperature, pH, and other parameters. So, the degree of swelling of hydrogels can be influenced by the temperature, pH and other parameters.[29] Hydrophobic interactions play an important role in the molecular mechanism of shape-changing
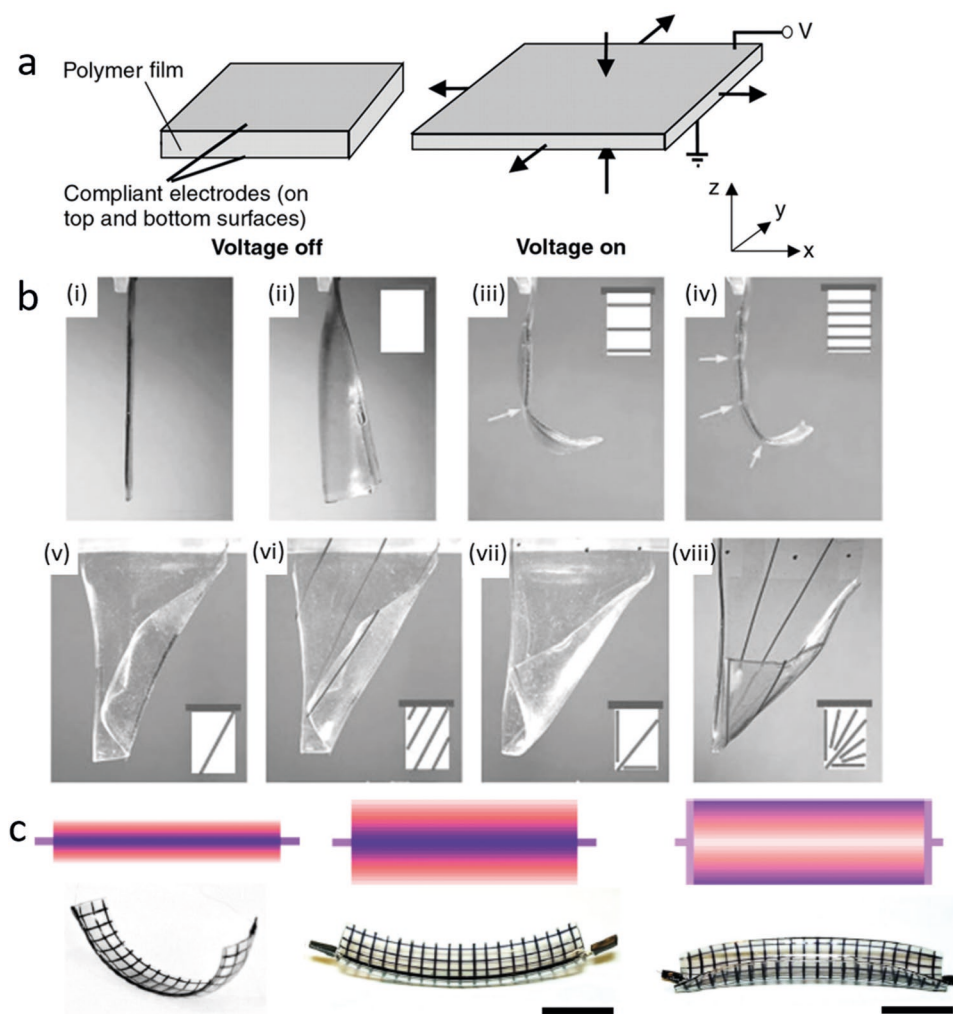
**ADVANCED
SCIENCE NEWS**
www.advancedsciencenews.com

**ADVANCED
FUNCTIONAL
MATERIALS**
www.afm-journal.de

Figure 3. The actuation of dielectric elastomers: a) The linear expansion of the dielectric elastomer due to the production of electrostatic force in the presence of compliant electrodes on the elastomer film, Reproduced with permission.[21] Copyright 2000, American Association for the Advancement of Science; b) the actuation of a bilayer structure of dielectric elastomer and fibers. i) The side view of the bilayer, ii) the actuation without fibers, iii,iv) side of bending of the bending actuation of the bilayer in presence of different number of fibers, v–viii) the bending behavior with varying number and arrangement of the fibers in the bilayer structure, Reproduced with permission.[24] Copyright 2015, Wiley-VCH.; c) demonstration of morphing behavior of a dielectric elastomer with the width of the electrode. The flat sheet of the elastomer produces torus structure with positive curvature when the width of the electrodes decreases from bottom to top. However, the reverse phenomenon takes place when the width of the electrodes increases gradually from bottom to top. The scale bar is 20 mm. Reproduced under the terms and conditions of the Creative Commons CC BY 4.0 license.[26] Copyright 2019, The Authors, published by Springer Nature.

hydrogels. The cooling induced segregation of polymer chains in a hydrophilic medium in the presence of hydrophobic interaction and further heating induced dissociation of aggregations of the polymer chains collectively triggering the shape-changing behavior in some temperature-sensitive shape-changing hydrogels.[30] (**Figure 4**a) The hydrophobic interaction provides addition crosslinking, which helps in fixing the temporary shapes. Further, the loss of this additional crosslinking at elevated temperature provides sufficient energy to recover the permanent shape. Apart from thermal stimulation, sometimes the complexation between the metal ion and organic moiety can also trigger the shape-changing behavior in hydrogels.[31,32] The additional crosslinking provided by the complexation between the metal ion and organic moiety helps in obtaining the temporary shape in shape-changing hydrogels. Further, the changing

in the oxidation state of the metal ion in the presence of external stimuli triggers the shape recovery process through the elimination of the additional crosslinking. (Figure 4b) In some cases, reversible supramolecular interactions such as host–guest interactions, red-ox interaction or antigen–antibody interactions triggering the shape fixing process producing some additional crosslinking in the hydrogel. Again, the elimination of that crosslinkings in the presence of pH or antigen stimuli helps in recovering the permanent shapes, as observed in Figure 4c.[33–36]

2.4. Nonuniform Strain (Liquid Crystal Elastomer)

Anisotropic shape changing in response to an external stimulus is a widespread phenomenon in liquid crystal elastomers
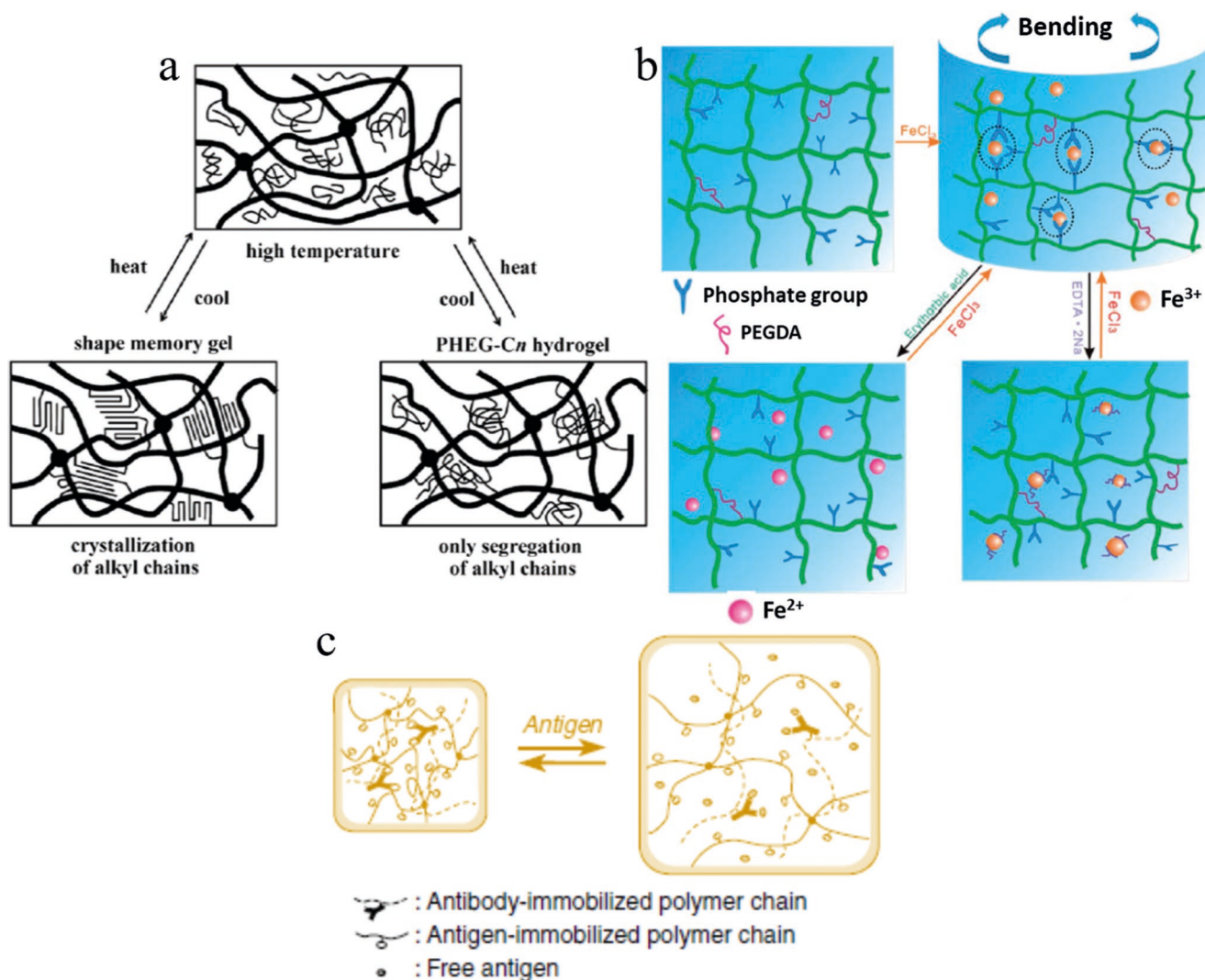
**ADVANCED
SCIENCE NEWS**
www.advancedsciencenews.com

**ADVANCED
FUNCTIONAL
MATERIALS**
www.afm-journal.de

Figure 4. The different shape-changing mechanism in hydrogels: a) The hydrophobic interaction induced aggregation of side chains of polymers, triggering the shape-changing behavior in hydrogels, Reproduced with permission.[30] Copyright 2012, Elsevier. b) The change in the degree of crosslinking due to the change in the oxidation state of the metal ion in presence of stimulus, triggering shape-changing phenomenon, Adapted with permission,[31] Copyright 2014, Royal Society of Chemistry; c) according to this molecular model, the antigen-induced change in the crosslinking density responsible for the reversible actuation in hydrogel; Reproduced with permission.[36] Copyright 1999, Springer Nature.

(LCEs). LCEs belong to a unique class of materials with properties of elastomers (entropic elasticity) as well as liquids crystals (self-organization).[37,38] LCEs are capable of remembering their previous state after phase transformation in the presence of stimuli, which enable them to contract and expand reversibly.[39–41] In the presence of the weakly crosslinked network, liquid crystal elastomers represent a state in between solids and liquids. Further, they have long-range orientational ordering due to the mesogenic moieties. Hence, under applied stress, a curvature elasticity along with deformation of this order is observed in liquid crystal elastomers. The combination of these two physical properties in a material help in emerging a qualitatively new state of matter in which the mesogenic polymer chains are capable of continuous orientational ordering because of the high molecular mobility of the polymer chains. Further, the mobile nature of the axis of orientational

symmetry breaking allows it to respond against applied elastic strains, and the whole system behaves like a Cosserat medium in which internal torques are permissible, and therefore, elastic stress may be nonsymmetric.[42] According to the molecular model of nonuniform deformations within the elastic limit of LCEs, developed by Trentjev et al., the free energy of deformations is a function of large nonsymmetric affine strains in the rubbery network and gradient of curvature deformations in the director field. Further, the elastic constants for the nonuniform directors in the presence of elastic strain depends on the polymer step length anisotropy.[42] Again, de Gennes et al. suggested a strong uniaxial deformation in LCEs without any significant change in volume, in response to a decrease in temperature across the isotropic to liquid crystal transition, is due to the change in the orientational order of liquid crystals.[43] Later, Finkelmann and Kundler reported that the nematic to
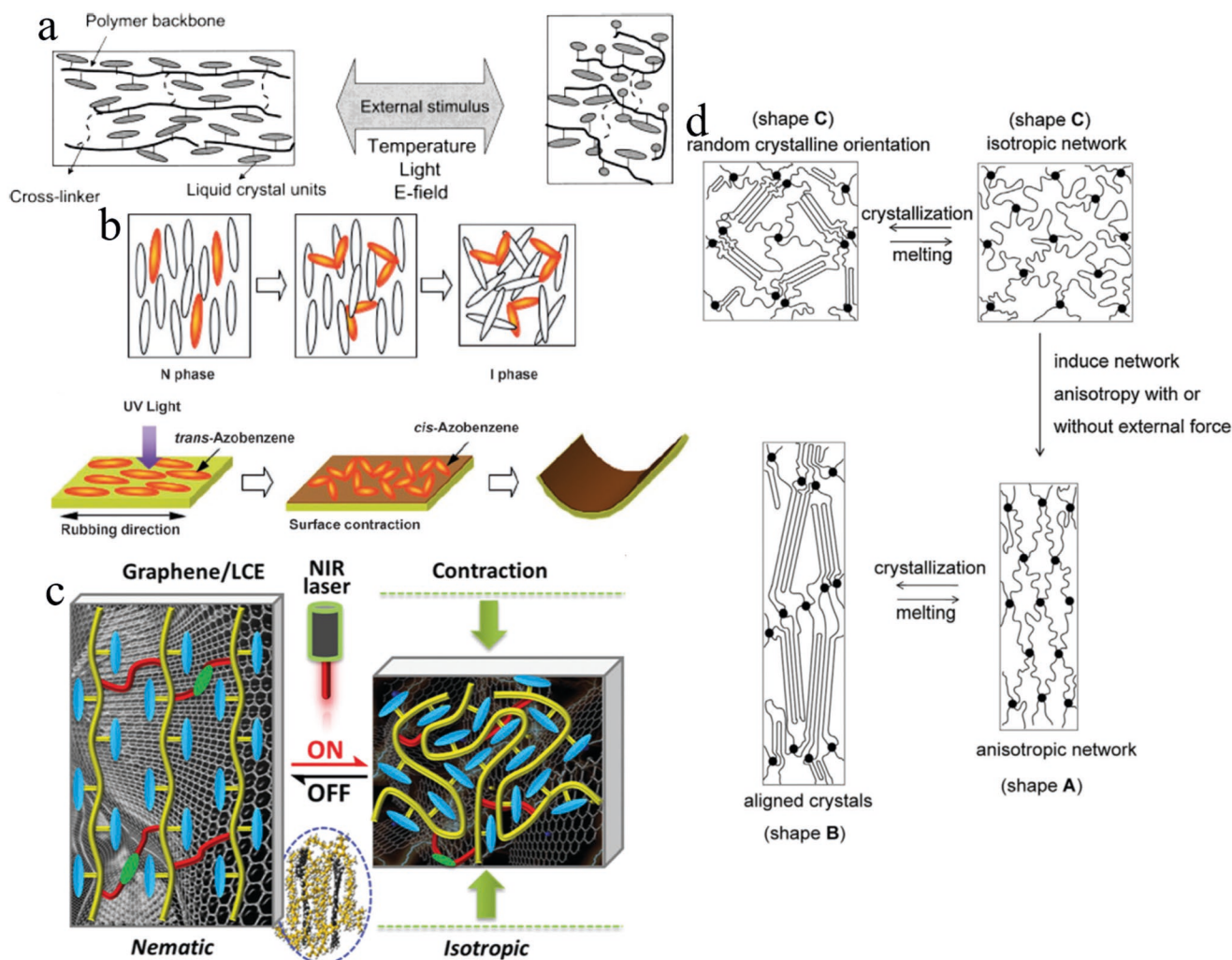
Figure 5. Nonuniform strain-induced shape-changing behavior: a) The processing induced (electrospinning) organization of the liquid crystal mesogens provides sufficient energy for showing shape actuation through anisotropic strain recovery, Reproduced with permission.[41] Copyright 2003, American Chemical Society; b) the photoisomerization of the surface liquid crystal domains of the LCEs due to limited absorption of light results self-folding of the shape through nonuniform strain recovery, Reproduced with permission.[49] Copyright 2006, Wiley-VCH; c) the photothermal property of graphene and hot stretching induced self-organization combined to trigger the shape-changing phenomenon, Reproduced with permission.[47] Copyright 2015, Wiley-VCH; d) the stretching induced organization of the molecular sheets improves the crystallization behavior of the materials, which trigger the anisotropic reversible shape-changing behavior in conventional polymers. Reproduced with permission.[8] Copyright 2015, Elsevier.

isotropic phase transition in LCEs is the driving force behind the temperature-induced spontaneous deformation along the director axis.[40] Naciri et al. prepared LCEs fibers with the side-on attachment of the liquid crystal mesogens.(**Figure 5**a) The processing induced alignment of the mesogen groups along the axis of the fiber allow the anisotropic contraction of the fiber along the fiber axis in the presence of external stimuli through the disorganization of the mesogenic groups.[41] Pei et al. reported the actuation behavior of liquid crystal elastomers with transferable crosslinking. The actuation process follows an alternative mechanism for mechanical relaxation. LCEs produce high alignment of liquid crystals instead of external stress relaxation through the creep of nonliquid crystal temporary framework with transferable links.[44] Ikeda et al. reported photo-induced 3D anisotropic deformation in LCEs

(Figure 5b) containing the azobenzene derivatives as liquid crystal mesogens and swollen in a solvent or heated above the glass transition temperature.[45] The azobenzene groups are sensitive to light and show photoresponsive *cis–trans* isomerization on exposure to light, which causes a significant change in length.[46] The limited absorption of light allowing only the surface mesogens to show photo isomerization which leads to the bending or 3D deformation in the developed materials. Further, a near-infrared spectroscopy responsive reversible mechanical actuation is achieved in graphene/LCE nanocomposite, where the graphene acts as photoactive constituents.[47] The in situ UV photopolymerization along with concurrent hot stretching organizes of the liquid crystal mesogens, and the extensive interactions between the graphene and mesogens allow the graphene sheets to distribute uniformly in the matrix. Now, the

**ADVANCED
SCIENCE NEWS**
www.advancedsciencenews.com

**ADVANCED
FUNCTIONAL
MATERIALS**
www.afm-journal.de

photothermal effect of graphene along with the high self-organization of the mesogens collectively trigger the photoresponsive reversible actuation phenomenon in nanocomposite (Figure 5c) and entropy driven elasticity is the driving force behind this large reversible deformation in the reported LCE which is one of the advantages of this material over other conventional polymeric materials.[48]

Apart from LCEs, some conventional polymers are also able to show anisotropic shape-changing behavior. Lendlein's group reported a thermoresponsive reversible bidirectional shape-changing phenomenon in a block copolymer made of polycaprolactone (PCL) and poly(ω-pentadecalactone) (PPD) building blocks[50] and proposed a molecular mechanism that triggers the reversible shape-changing phenomenon (Figure 5d). Shape C is the permanent shape of the polymer in which the polymer chains are randomly oriented. The programming through uniaxial deformation changed the conformation of both the crystalline domains (PCL and PPD), as observed in shape A. Further, the heating–cooling cycles allow only the PCL domain to melt or crystallize while the PPD domain remains unchanged and produce the network anisotropy for PCL domain without external force. Overall, the programming induced conformational anisotropy deforms the PPD domain, and the constrain produced by the deformed PPD domain helps the PCL domain to be in oriented conformation.[51] The crystallization induced elongation and melting induced contraction of the length with heating–cooling cycles along the programming axis produces the reversible shape-changing behavior in this material.

2.5. Surface Tension

Surface tension or the capillary force becomes a very relevant and dominating driving force for showing shape-changing behavior in soft materials or materials with small dimensions as surface force starts to dominate over the bulk force of gravity at a smaller level.[52] Sometimes, this surface force is so strong that it destroys the thin structure of micro or nanoscale devices.[53] There are many reports in which the capillary action or surface tension functions as the driving force for shape-changing behavior or arranging and adjusting the 2D rigid objects at the surface of the water.[54] To understand the relative importance of surface energy with respect to bulk elasticity, a liquid droplet with surface tension γ is considered over an ideal smooth and uniform solid surface.[55] (**Figure 6**a) After deposition, the droplet makes an angle θ with the surface of a rigid substrate, which is classically adjusted through a balance among all surface forces at the interaction line. If the typical extent of deformation at the pinched region is δ, then it can be defined by Equation (2)[56]

$$\delta \sim \frac{\gamma}{E}\sin\theta \qquad (2)$$

where, E is the elastic modulus of the material, and $\gamma \sin\theta$ is the vertical component of surface tension, which helps in deforming the substrate by pulling the substrate.[57] Further, consider an elastic plate (length L, width w, and thickness h) coated with a thin liquid layer with surface tension γ. The contact of this plate with a rigid cylinder (radius R) coated with same liquid layer
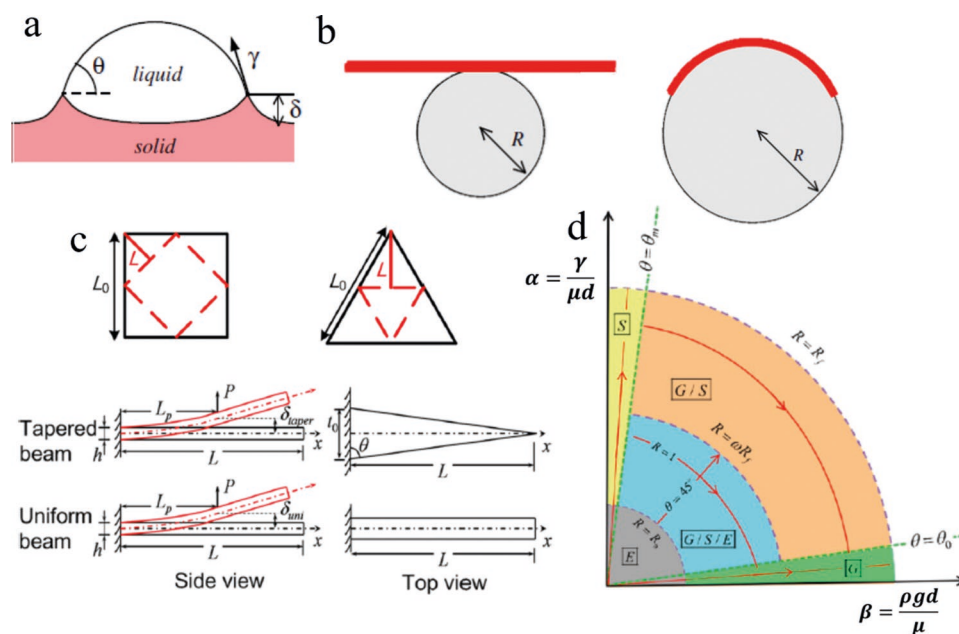

Figure 6. Surface tension as the driving force in shape-changing behavior: a) Model describing surface deformation at the solid–liquid interface due to surface tension, Reproduced with permission.[55] Copyright 2008, American Chemical Society; b) the model helps in optimizing different responsible factors for bending of an elastic plate (red color) in contact with any cylinder (both coated with a thin layer of liquid), Reproduced with permission.[58] Copyright 2010, Institute of Physics Publishing; c) according to this model, the self-folding is driven by the capillary interactions at the triple junction; the symmetric red dash line denotes the bending point in both square and trigonal schematic models, Reproduced with permission.[59] Copyright 2009, United State National Academy of Science; d) the deformation map describing the role of elasticity (*E*), gravity (*G*), surface tension (*S*) in defining the shape of a soft material. Reproduced with permission[60] Copyright 2013, Amerian Chemical Society.

leads to the wrapping of the cylinder by the plate (Figure 6b) which results in enhancement not only in the surface energy by $2\gamma wL$ but also in the elastic energy by $BwL/2R^2$; where B is the bending modulus of the elastic plate and $B = Eh^3/12(1-\nu^2)$, E and ν are the elastic modulus and Poisson ratio of the materials. Hence, the wrapping is only possible if the radius of the cylinder $R > \frac{\sqrt{B/\gamma}}{2^3}$; where $\sqrt{B}/\gamma = L_{EC}$ (elasto-capillary length). So, the characteristic length of the flexible plate should be less than the radius of the rigid cylinder for spontaneous wrapping.[58] Guo et al. reported the self-folding behavior of thin-film single crystal silicon and proposed a mechanics model identifying the responsible parameter.[59] According to this model, the folding behavior of the thin film is driven by the capillary interaction at the triple junction. Figure 6c shows that the thin sheets are like tapered cantilever beam and the capillary force works on the beam at a particular position (L_p) with an extent of γt where t is the width of the beam or length of the contact line at L_p and this capillary force should be enough to overcome the bending resistance of the beam for self-folding of the thin films. A deformation map is proposed by Xu et al. to understand the influence of different parameters on the surface tension drove shape-changing behavior and to optimize difference influencing factors for successful folding.[60] The map is prepared using polar coordinate system and considering two extreme conditions; i) in which the deformation is exclusively driven by the surface tension and the overall strain due to the surface tension is in the order of $\alpha = \gamma/\mu d$, μ is the shear modulus and d is the length of the axis, and ii) in which the gravity is the dominating factor and average strain is in the order of $\beta = \rho g d/\mu$ where the ρ is the mass density and g is the gravitational force. (Figure 6d) The map is divided into five region depending on the role of the elasticity (E), gravity (G), and surface tension (S) in defining the shape of the material.

3. Principles of Complex Shape Transformation

The shape-changing behavior of polymeric materials can be precisely programmed by their geometry and structure. Here, we discuss how different kinds of complex actuations are realized in different shape-changing materials. [87]

The folding behavior of a material can be defined as deformation of a material keeping the in-surface distance between the two distinct points of the material without self-intersections.[88] The folding is a sharp curvature of the material, which results due to the deformation of the material along a crease and produces a narrow hinge area with sharp angles.[89,90] Folding can be achieved in a material utilizing the stress mismatch between the active and passive layers.[91–93] For example, the hinge printed with active materials (shape-changing material) and other parts printed with inactive materials results in folding in the presence of the appropriate stimulus. The 4D printed structure developed by Tibbits folds into a precisely truncated octahedron in the presence of water stimuli.[94]

Bending can be defined as the disseminated deformation in the material throughout the deflected area resulting in curvature in the material.[89,95] Bending can be achieved by attaching two materials with different degrees of swelling or shrinking

behavior. The bilayer structure will bend to keep equal strain at the interface of the bilayer on activation by the stimuli.[93] Zhang et al. fabricated a lightweight 3D composite structure that remains flat on heating due to the release of internal strain but starts to bend on cooling to room temperature.[96] There is some basic difference between folding and bending, such as folding results due to localized deformation while bending happens due to global deformation in the material.[97] Further, in the presence of continuously applied force during bending, the shape changing results rolling deformation in the material. The main difference between bending and rolling is rolling consists of multiple gradients while bending consists of only two gradients.

Twisting behavior can be achieved in a material by using in-plane stretching. The combination of two anisotropic active layers of a similar kind with stretching direction perpendicular to each other results in self-twisting in the bilayer structure. Shape changing material with a small width is favorable for showing twisting behavior.[98] The printing of fibers with certain angle results twisting in shape.[96]

Helixing can be characterized by the smooth distortion of the material in space, which results in a three-dimension curvature.[92] Helixing deformation can be achieved in a bilayer structure through the uniaxial stretching or shrinking of the active layer with a nonzero angle between the axis of stretching and the axis of bilayer structure.[99] The basic difference between twisting and helixing is that the axis of twist is centered in twist shape while helixing possesses multiple axes.

The buckling deformation can be achieved by the application of compressive stress above a critical value, which results in sudden sideway failure in a flat structural membrane.[100] The compressive stress can be generated through the in-plane organization of different active and passive elements. Menan et al. discussed four different ways, such as material tessellation, in-plane material gradients, nonhomogeneous exposure to stimuli and application mechanical stress, to generate buckling deformation.

Curving can be defined as the deviation in the geometry of an object from its plane or flat shape. This type of shape-changing behavior can be achieved through the unequal stress generation in between the active and passive layer. The different degrees of swelling of two layers in the presence of stimuli can produce unequal stress in the material.[94] Further, the stress gradient could be generated by the application of varying intensity of the stimuli along with the thickness of the material.[101]

The topographical changes can produce distorted or uneven shape in the material, which is quite similar to the physical properties of ground terrain. The surface topography can be defined as the local deviation of a surface from its flat plane. The concentric circles in the presence of suitable stimuli produce mountain and valley-like features.[102] Further, it can also be realized under compressive loading.[94]

The unequal swelling/shrinking behavior of a bilayer structure with similar stiffness and layer thickness results in wave or curling shape in response to an appropriate stimulus.[94,103] The basic difference between waving and curling is the consistency of the wave after distortion. Further, curling possesses irregular curves while waving consists of more symmetric curves. The wave shape can be tuned by changing the position and

**ADVANCED
SCIENCE NEWS**
www.advancedsciencenews.com

**ADVANCED
FUNCTIONAL
MATERIALS**
www.afm-journal.de

materials of each layer. The trilayer structure developed by Wu et al. consists of an active layer of SMP and two passive layers. The heating induced activation of SMP of the trilayer structure results in a wave shape.[93]

3.1. Complex Deformation of Stress Relaxation-Based Shape-Changing Polymers (Shape Memory Polymers)

Complex shape changing in SMPs is highly associated with the complex programming of the permanent shape of the SMPs into temporary shape, and different kinds of stimuli can play an important role in executing this complex shape-changing phenomenon.[104,105] Thus, complex actuation in shape-memory polymers can be achieved without structuring but by their deformation. This not only increases the versatility of programming as well as helps in predicting the pathway.

Exposure to the whole sample to conditions when which polymer chains become mobile results in simultaneous actuation of all parts of a sample—it simply returns to its initial shape. Sequential folding can be achieved when samples are exposed to localized stimuli such as light. Indeed, heating of sample with laser light allows site-specific shape transformation, which is determined by the permanent shape. For example, the photothermal or magnetothermal effect of nanoparticles or dyes can play an important role in the production of heat in the presence of light or magnetic field.[106,107] The more advance complex programming can be achieved using the light of different wavelengths, which produces heat after absorbing light selectively by some special dyes.[108,109] Liu et al. developed a simple method to show complex shape changing in a prestrained polymer sheet. They printed ink using a desktop printer onto the polymer sheet, and irradiation with light allows the printed zone to produce heat which triggers the gradient shrinking of the polymer chains across the thickness of the polymer sheet. This shrinkage causes the polymer sheet to fold immediately.[106] Similarly, sequential folding can be achieved by printing different color ink over the polystyrene sheet and then irradiate the polymer sheet with LED light of particular color to trigger the folding process. **Figure 7**a shows the sequential folding of a nested box on exposing to red and green light, respectively, on which red and green ink is printed with a desktop printer. The folding of the nested box taking place due to the photothermal effect produced by the inks printed over it.[108]

Another way to achieve complex deformation of shape-memory polymers is to use a multicomponent object. For example, the electromechanical or thermos-mechanical shape changing can be achieved after programming the composite utilizing its broad glass transition temperature.[110] This composite acts like an ion polymer–metal composite and the transportation of ions and water molecules along with the electrostatic force under the influence of applied voltage, trigger the electromechanical shape-changing phenomenon in this composite. Simultaneous application of temperature and electric stimulus helps the composite material to show very complex shape transformation behavior, as observed in Figure 7b. The temperature triggers the twisting and bending while the electric field activates the oscillation. Tolley et al. reported a complex shape-changing phenomenon of shape memory polymer composite under uniform heating.[111] The polymer composite is fabricated by putting the prestrained SMP in between two papers, as observed in Figure 7c. The heat-induced contraction of the SMP resulting bending in the laminate structure, perpendicular to the axis p and toward the gap until the two sides of the upper layer come in contact, fighting against the force of gravity at the free end. Although multilayer shape memory polymers have some advantages like good and easily tunable elastic properties, although their fabrication is still time-consuming and complex in nature. To overcome this issue, Jin et al. developed a crystalline shape memory polymer with thermo and photoreversible bonding to produce complex shape actuation.[112] In this case, two different responsibilities are assigned to two different reversible bonding. The network anisotropy and location of actuation are generated through the activation of photoreversible bonding in a spatial-selective manner while shape-memory behavior is controlled by the thermoreversible bonding. The combination of the effects of these two different type of reversible bonding triggers complex shape transformation, from simple 2D films to 3D structures (Figure 7d).

3.2. Complex Deformation of Shape-Changing Polymers with Volume Change (Hydrogels)

In most cases, the hydrogels and other volume changing polymers exhibit shape-changing behavior because of their isotropic volume expansion and contraction in response to a stimulus. Complex shape changing such as bending, twisting, and folding can be achieved by inhomogeneous expansion or contraction of the material in different directions.[113] At the end, the way how shape-transformation occurs depends on the structure of hydrogel. For example, the bending behavior can be produced through the introduction of bilayers of two different polymeric materials with different expansion co-efficient while the twisting behavior can be achieved using bilayers of different materials with gradually changing thickness ratio between two layers. Twisting is achieved when the ratio between the thickness of parts with different swelling properties changes gradually along with the sample.

More complex actuation can be achieved when several bilayer elements are combined with each other and with nonactuating parts. Small bilayer connected to nonactuating elements can be used to introduce sharp edges. The curvature of the edge is determined by parameters of the bilayer, and the bending angle also depends on the size of the bilayer. **Figure 8**a shows that the attachment of the bilayer structure in the structure of film triggers the formation of hinge shapes. The bilayer structure is patterned using noncontact photolithography of the hydrogel which is composed of N-isopropyl-acrylamide (NIPAm), acrylic acid (AAc), and poly-ethylene oxide diacrylate (PEODA). The "Venus Flytrap" shape reversible closes and opens with changing the pH due to different degrees of swelling of the two different layers.[114] Similarly, patterned polymer film with areas of different swelling magnitude results in similar phenomena.

Bilayers can bend in one direction that restricts possibilities for microfabrication. Hayward and co-workers have proposed a very interesting solution to this problem—they have fabricated
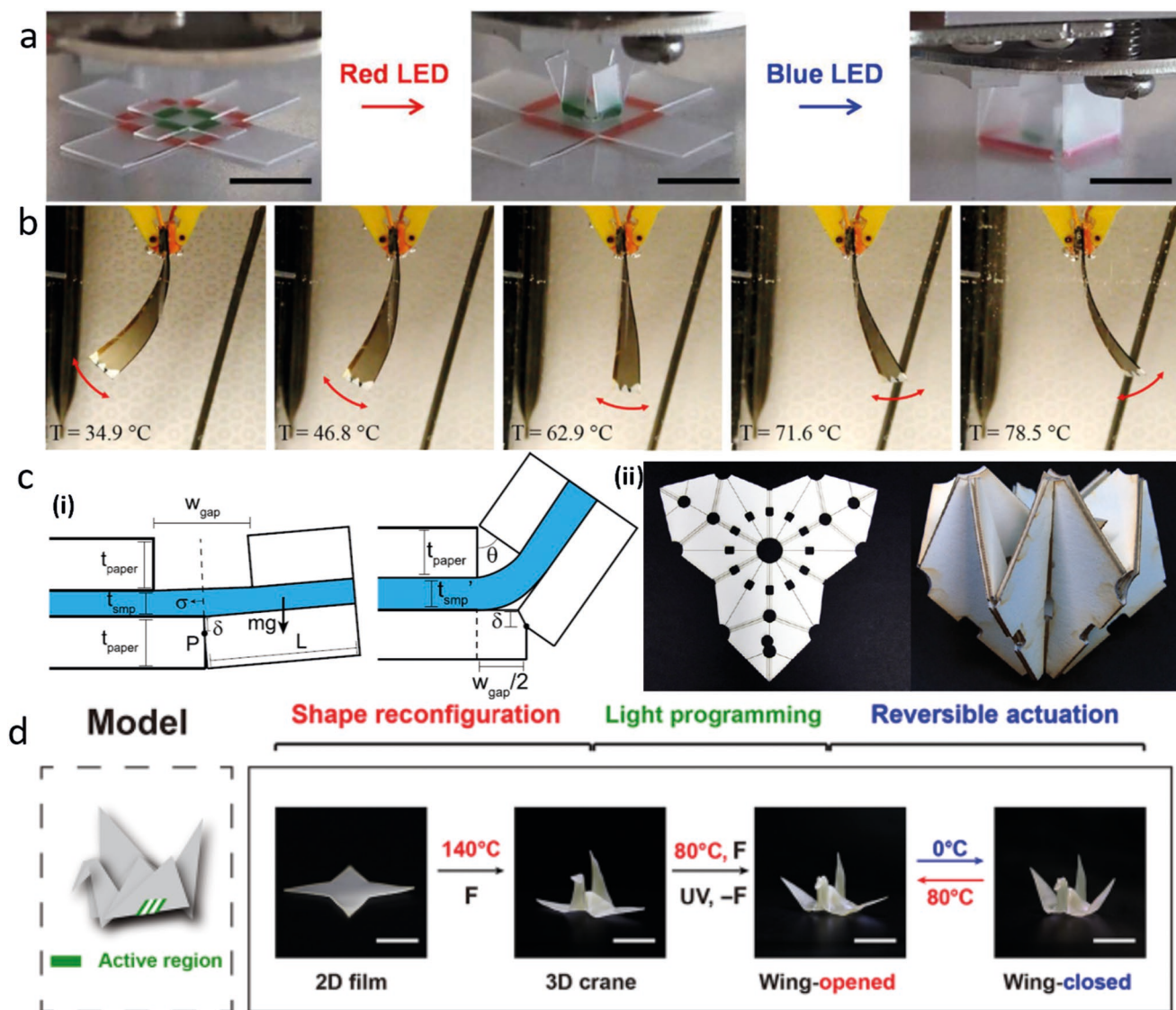
ADVANCED
SCIENCE NEWS
www.advancedsciencenews.com

ADVANCED
FUNCTIONAL
MATERIALS
www.afm-journal.de

Figure 7. Complex shape-changing behavior of shape memory polymer through stress relaxation: a) The sequential shape-changing behavior of a SMP coated with different dyes, which activate the shape-changing behavior using photothermal effect, Reproduced with permission.[108] Copyright 2017, American Association for the Advancement of Science; b) the oscillation of the shape of a multiple SMP-metal composite is observed in presence of constant electric field (a sinusoid AC voltage of 3.7 V initial amplitude and 1 Hz frequency) and with varying temperature, Reproduced under the terms and conditions of the Creative Commons CC by 4.0 license.[110] Copyright 2016, Springer Nature; c) the active layer of SMP sandwich between two inactive layers of paper folds perpendicular to the *p* until the sides of the two-layer touches with each other i). The self –folding behavior of a trilayer structure due to the contraction of SMP layer on activation ii), Reproduced with permission[111] Copyright 2014, Institute of Physics Publishing; d) the thermo and photo reversible bonding triggers the complex 2D to 3D shape transformation in a SMP. Reproduced with permission.[112] Copyright 2018, American Association for the Advancement of Science.

trilayer structure when the top and bottom layers do not swell, and the middle layer is a stimuli-responsive hydrogel. Bending to one or another side can be achieved when either top or passive bottom layers are missing. The patterned sheet developed by Hayward and his co-worker using pendent benzophenone containing poly(*N*-isopropyl acrylamide) copolymers showing self-actuating behavior on changing temperature (Figure 8b). The heating (49 °C) induced deswelling, recover the flat shape while cooling (22 °C) induced swelling helps to obtain the initial hybrid shape.[115] Figure 8c describes the folding behavior of the trilayers structure in which the active hydrogel layer is

sandwiched in between two passive layers, and the small gaps in the upper or lower side help the trilayer structure to bend in one or other side. The photo-crosslinkable trilayer pattern structure developed by Na et al. shows reversible complex shape-changing behavior utilizing temperature-dependent swelling/deswelling behavior of the active hydrogel layer.[116] Another way of achieving folding behavior is to use the swelling pathways, which are determined by the shape of the film, as observed in Figure 8d. In which, a six-ray star-like bilayer structure of poly(*N*-isopropyl acrylamide-*co*-acrylic acid) (P(NIPAM-AA) and poly-(methyl methacrylate) (PMMA) shows complex
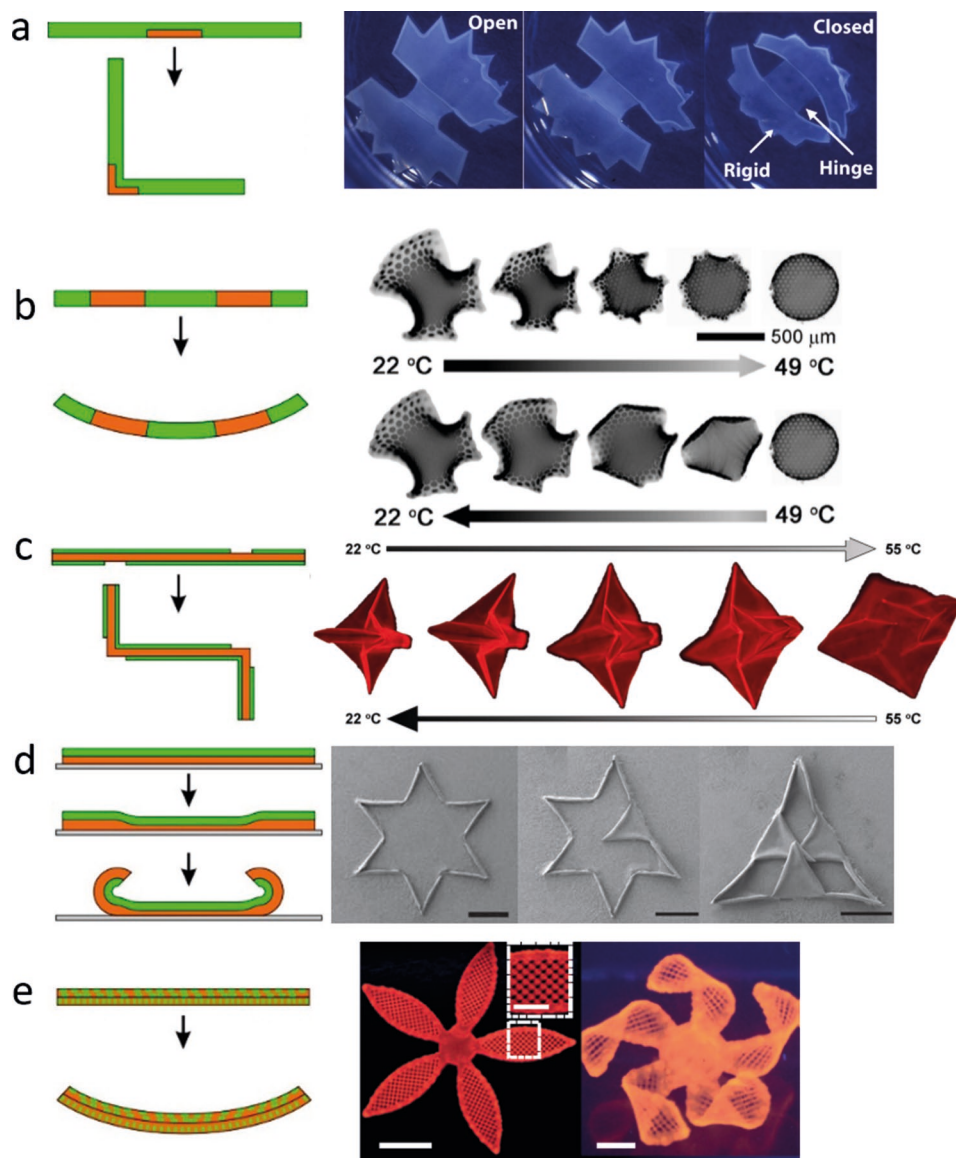
**ADVANCED
SCIENCE NEWS**
www.advancedsciencenews.com

*ADVANCED
FUNCTIONAL
MATERIALS*
www.afm-journal.de

Figure 8. Various strategies to introduce complex shape changing in polymers by using structure: a) pattern bilayer: reversible actuation of "Venus Flytrap" shape of bilayer hydrogel of poly (*N*-isopropylacrylamide-co-acrylic acid)/poly(ethylene oxide) diacrylate (NIPAm–AAc/PEODA) with pH change, Reproduced with permission.[114] Copyright 2010, Elsevier; b) patterned film: reversible shape-changing behavior of hydrogel of pendent benzophenone containing poly(*N*-isopropyl acrylamide) copolymers. The heating induced deswelling helps to get the flat structure while cooling induced swelling produces the initial structure, Reproduced with permission.[115] Copyright 2012, American Association for the Advancement of Science; c) the heating leads to deswelling and cooling induced swelling of photo crosslinkable trilayer pattern structure triggers the reversible self-folding phenomenon, Reproduced with permission.[116] Copyright 2015, Wiley-VCH; d) self-folding behavior of a star shape bilayer structure though the edge activation, Reproduced with permission.[117] Copyright 2013, Wiley-VCH; e) the complex changing behavior due to anisotropic swelling behavior of composite. Reproduced with permission.[95] Copyright 2016, Springer Nature.

multistep folding through edge activation.[117] Further, the introduction of anisotropic volume expansion using either fibers or platelets can produce complex shape changing in a material (Figure 8e)).[118] Gladman et al. reported the complex shape-changing behavior of a polymer composite due to anisotropic swelling behavior. The processing induced alignment of the cellulose fibrils controls the swelling of the composite and results in complex 3D morphologies in the presence of the stimulus.[95] The extent of bending depends on the elastic modulus, swelling ratio, thickness ratio of the layers ($m = a_{bottom}/a_{top}$), and the

total thickness of the bilayer ($h = a_{top} + a_{bottom}$). The mean and Gaussian curvatures scale, respectively

$$H = c_1 \frac{\alpha_\parallel - \alpha_\perp}{h} \frac{\sin^2\theta}{c_2 - c_3\cos2\theta + m^4\cos4\theta} \text{ and}$$

$$G = c_4 \frac{(\alpha_\parallel - \alpha_\perp)^2}{h^2} \frac{\sin^2\theta}{c_5 - c_6\cos2\theta + m^4\cos4\theta} \qquad (3)$$

where, the c_1, c_2, c_3....etc. are the elastic constants that are assigned by their swollen equilibrium value. Hence, there are

variety of possibilities to produce complex shape-changing behavior in hydrogel-based systems.

3.3. Complex Deformation of Shape-Changing Polymers with the Nonuniform Strain (Liquid Crystal Elastomers)

Complex shape-changing behavior in liquid crystal elastomers can be attained either through in-depth or/in-plane variation of molecular orientation[119–124] or by using photoresponsive mesogens, which are capable of deforming upon irradiation with light.[125,126] Hence, folding in liquid crystal elastomers can be controlled by organized irradiation with light and by controlling the distribution of molecular directors. van Oosten et al. reported complex shape-changing behavior in an LCE containing two different dyes (A3MA and DR1A).[119] It is explored that the self-organization and anisotropic orientation of mesogens controlling complex folding. According to **Figure 9**a(i), a gradual change in the orientation of the mesogen units with the thickness of the materials, a parallel orientation in the top

to a perpendicular orientation at the bottom with respect to the substrate at bottom. This type of splayed molecular orientation is controlling not only the folding direction but also the axis of folding of the film. Different complex folding is achieved using varying compositions of the two dyes and using the light of different wavelengths and different compositions. (Figure 9a(ii)) In the dark, no folding is observed, but in the presence of ultraviolet light, the yellow part responsible for A3MA dye starts bending. At the same time, the red part responsible for DR1A dye remains unbent. Again, in the presence of visible light, the reverse phenomenon is observed; the red part starts bending while the yellow part remains unbent. Finally, in the presence of both UV and visible light, a flap bending throughout the length is observed because of the simultaneous absorption of light by the DR1A at 360 nm and A3AM at 440 nm. So, the switching between these four states in the presence of different light generates cilia motion. Haan et al. introduced complex shape-changing behavior in LCEs through the developed of series 3D patterned structure of liquid crystal units. In the presence of appropriate stimuli such as pH or temperature, an
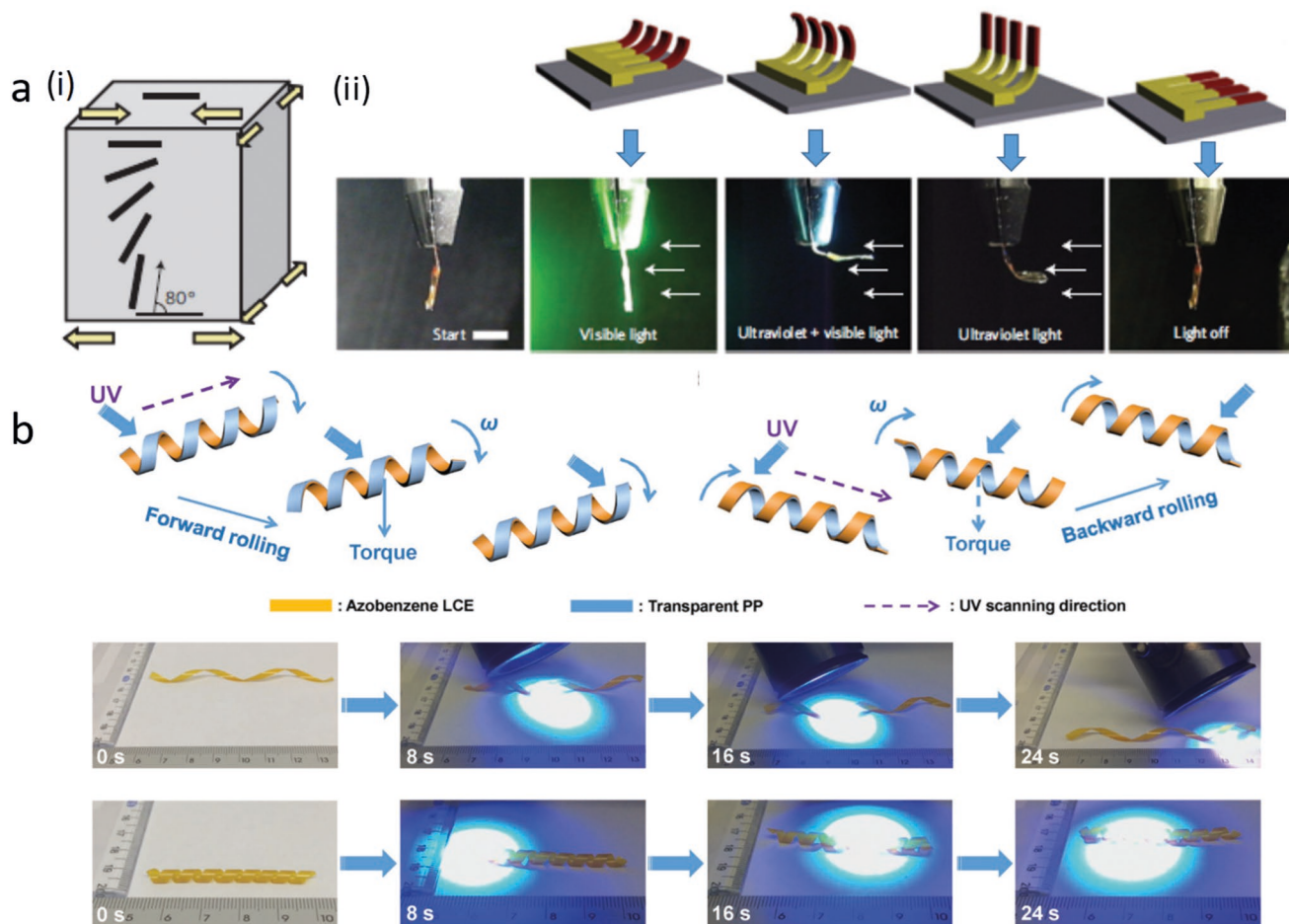

Figure 9. Complex shape changing due to nonuniform strain: a) The orientation of the liquid crystal units gradually changes from top to bottom in the LCE film i); The extent of bending of the film in the presence of different wavelength of light. The A3AM dye-containing yellow part bents in the presence of ultraviolet rays while the DR1A containing the red part of the film bents in the presence of visible light. A cilia motion is observed in the film on the simultaneous application of a different source of light ii), Reproduced with permission.[119] Copyright 2009, Springer Nature; b) forward and backward rolling motion of a spring-like motor, made of LCE inner side and outer side, respectively, due to the torque produced by structured irradiation with UV-light. Reproduced with permission.[125] Copyright 2017, Wiley-VCH.

accordion-like deformation can be achieved in a striped shape selecting the appropriate composition of the reactive mesogen mixture. A large deformation can be achieved through this type of out of plane shape changing by contracting a monodomain sample with the uniform nematic director.[124] A novel strategy has been introduced by Lu et al. to improve complex shape-changing behavior in LCEs by enhancing the photoinduced mechanical force.[125] The basic idea is to store the mechanical energy in the polymer backbone through deformation (such as stretching or twisting) and use that stored energy during the light-induced shape transformation. The irradiation with light not only produces mechanical force through the direct light to mechanical energy conversion upon *cis–trans* photo isomerization of the azobenzene liquid crystal unit as well as activate the release of the prestored deformation energy. The combination of these two forces helps in producing wheels or spring-like motors, as observed in Figure 9b. The motion in a spring-like motor is generated through the production of UV light-induced torque, while forward or backward direction of the motion depends on the processing of the bilayer structure of BOPP and LCE. When the LCE layer is in the upper side of the ribbon backward movement takes place while it is in the inner side of the ribbon reverse movement takes place.

4. Application of Shape-Transforming Soft Materials

Depending on shape-transforming material type, the principle of transformation and stimuli, these materials can be used in various fields like smart textiles, tissue engineering, soft robotics, microfluidics, sensors, drug delivery, optical devices, and electronic devices (**Figure 10**). All applications can be divided into several groups. Mechanical actuators and soft robotic systems belong to the first group and relay of both amplitudes of deformation and force generated during deformation (described by stroke-force dependence). Some applications utilize shape transformation to affect other properties. Examples of such applications are lenses (focal length is changed) and smart textiles (appearance and heat exchanges are changed). The third group of applications utilizes shape transformation to generate shapes, which otherwise are not possible or difficult to achieve. An example of such kind of application is tissue engineering.

4.1. Stroke-Force Dependence

4.1.1. Soft Robotics

Soft robotics is one of the fastest-growing fields of application for shape-transforming materials. In comparison to metal-based hard materials, soft materials offer multifunctionality and reconfigurability.[127] The use of soft materials in robotics, allow us to access small inaccessible regions, to manipulate delicate objects, and to have safe interactions with robotic design system.[128] Shape transforming soft materials are even more interesting for soft robotics applications than other soft materials, due to their shape change there is limited need for hydraulic or pneumatic pumps to actuate and induce the motion in the system. Shape transforming materials have
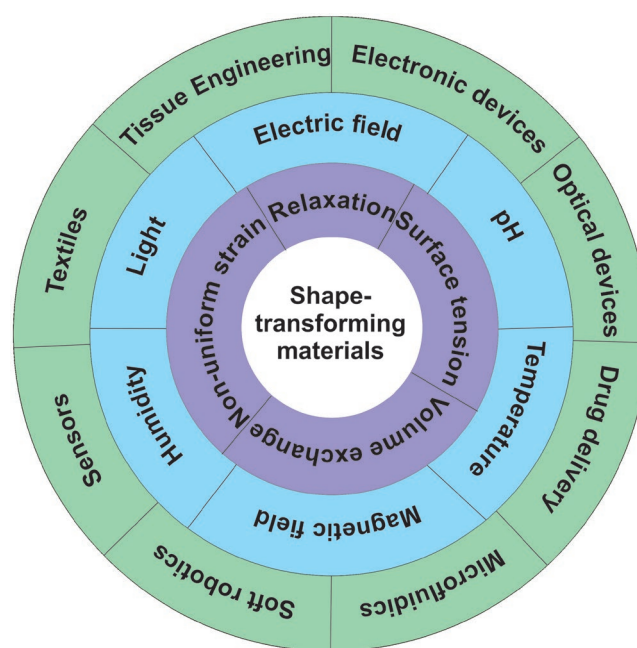

Figure 10. Scheme showing the shape-transforming soft material principle of transformation, stimuli, and applications.

showed that with proper design they can achieve such bioinspired locomotions as walking, jumping and swimming, which are solely based on their shape-changing characteristics.[129] As an example, Han et al. designed electroactive hydrogels that by changing the electric field was able to grip and transport objects and do bidirectional locomotion[130] (**Figure 11**a). By using digital light processing (DLP) based micro 3D printing technique, they were able to get various size 3D structures with high resolution, fast actuation and ease control. These kinds of hydrogels have the potential to be used as actuating material for artificial muscle design and soft robotics. Though there is one problem with this kind of soft robot, the electric field is required. One option to solve this issue and prepare wireless actuator that is controlled by using light. Huang et al. described light driven liquid-crystal soft robotic system where UV light and white light works as "power and signal lines"[131] (Figure 11b). Liquid crystal film was able to achieve shape transformation with light due to azobenzene molecules that are included in the film, with UV irradiation azobenzene molecules switch from *cis* to *trans* isomer that changes the length of molecule and induces bending of the film. The prepared soft robot was able to swim in water and carry loads. Light driven soft robots have potential to be used in micro machines and robotics .

4.1.2. Microfluidics

Fluid manipulation in channels with dimensions of tens of micrometers is called microfluidics; this field is constantly growing as it could improve various fields: chemical synthesis, biological analysis, optics, information technology, etc.[132] Microfluidic devices by itself is usually small in scale, whereas their
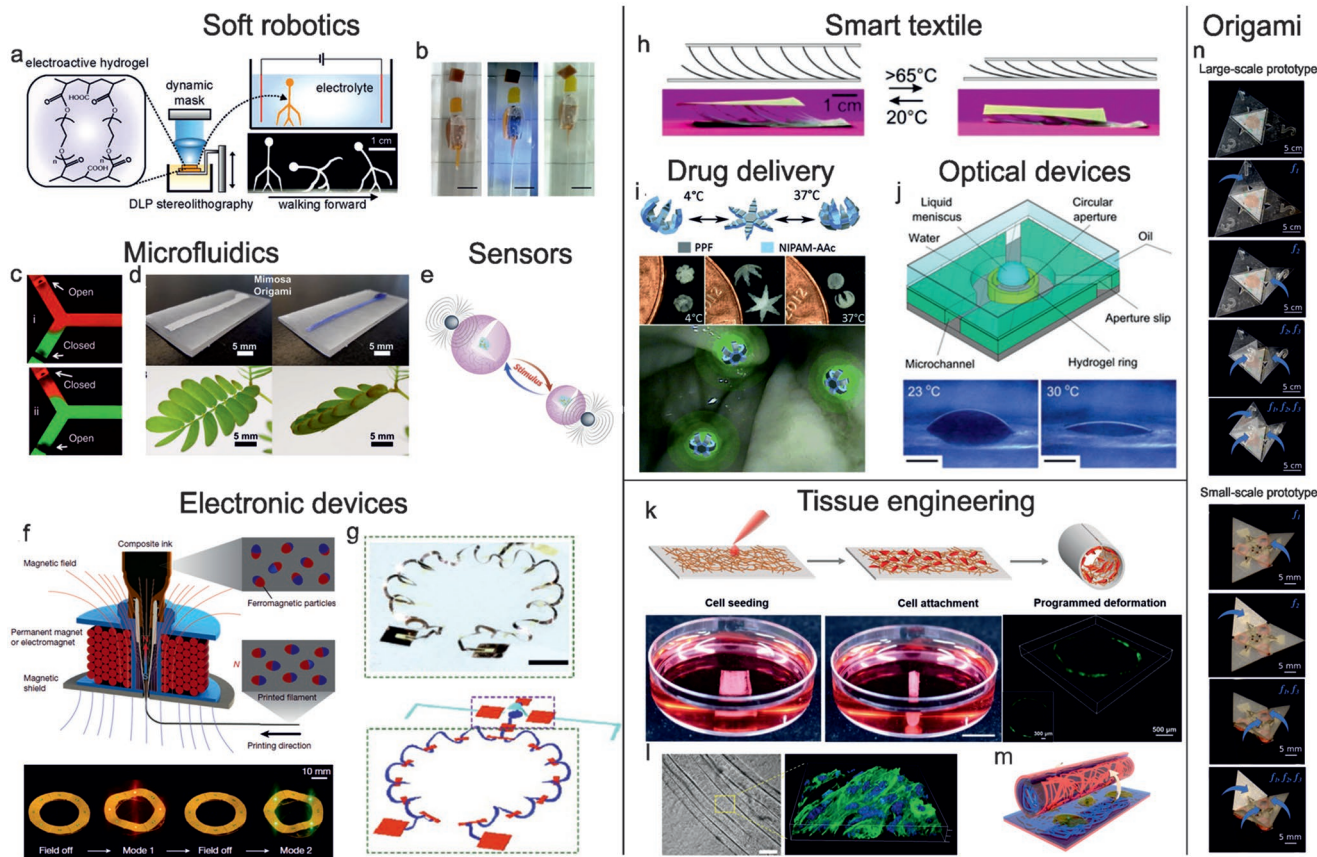
Figure 11. Overview of different application of shape-transforming soft materials: a) 3D printed electroactive hydrogel soft robotic manipulation and locomotion. Adapted with permission.[130] Copyright 2018, American Chemical Society; b) miniaturized swimming soft robot controlled by remote light signals. Scale bar 3 mm. Adapted with permission.[131] Reproduced under the terms and conditions of the Creative Commons CC BY 4.0 license.[131] Copyright 2015, Springer Nature; c) microfluidic actuators based on temperature-responsive PNIPAM hydrogels. Adapted with permission.[133] Adapted under the terms and conditions of the Creative Commons CC BY 4.0 License.[133] Copyright 2018, Springer Nature; d) Mimosa origami: self-organization of a rectangular-shaped Janus bilayer. Adapted with permission.[134] Copyright 2016, American Association for the Advancement of Science; e) hybrid sensor with temperature-responsive PNIPAM hydrogel as a spacing transducer. Adapted with permission.[138] Reproduced under the terms and conditions of the Creative Commons CC BY 4.0 license.[138] Copyright 2018, Springer Nature; f) 3D printed soft materials with programmed ferromagnetic domains. Adapted with permission.[139] Copyright 2018, Springer Nature; g) 3D morphable mesostructures for microelectronic devices. Adapted with permission.[140] Copyright 2018, Springer Nature; h) structures with switchable thickness based on Janus fibers for smart textile application. Adapted with permission.[144] Copyright 2017, American Chemical Society; i) stimuli-responsive theragrippers for chemomechanical-controlled drug release. Adapted with permission.[150] Copyright 2014, Wiley-VCH; j) smart optical lenses with tunable focal lengths based on PNIPAM hydrogel. Adapted with permission.[153] Copyright 2006, Springer Nature; k) shape morphing scaffolds for 3D endothelialization, photographs showing the temporary planar shapes (25 °C) and the permanent shapes (37 °C). Scale bar 1 cm., 3D tubular organization of HUVECs on the bilayer in permanent tubular shape (green color, stained by Calcein AM) cultured. Adapted with permission.[158] Copyright 2018, Wiley-VCH; l) bright-field image taken after 10 d of incubation of C2C12 cells in the internal part of the PEGDA tube and the 3D reconstructed confocal image of the partially aligned cells. Green and blue colors represent the cytoskeleton and cell nuclei, respectively. Adapted with permission.[159] Copyright 2018, Wiley-VCH; m) 4D biofabrication of porous tubular PCL/PNIPAM scaffolds. Adapted with permission.[160] Copyright 2017, American Chemical Society; n) Wireless folding of multijoint robots. Adapted with permission.[163] Copyright 2017, The American Association for the Advancement of Science.

equipment that is required to control the device could be large (pumps, valves, mixing units). Due to shape-changing properties and force that is generated during actuation, shape-transforming materials are well suited for valve preparation in microfluidic channels. For example, recently D'Eramo has shown the potential to use temperature-responsive hydrogel as poly(N-isopropylacrylamide) (PNIPAM) for microfluidic valves[133] (Figure 11c). At 40 °C (above LCST), PNIPAM hydrogel shrinks, but in the room temperature, hydrogel swells, closing the valve in this case. They have prepared 780 microcages, were able to open and close in 250 and 600 ms, respectively. They were able to

use these cages for single-cell handling and the nuclear acid amplification test (NAAT), which proves systems functionality for microfluidics. Another interesting approach is to fabricate stimuli-responsive microchannels that can be open and closed, used for bulb mixing, and can form U, T- junctions described by Wong et al.[134] (Figure 11d). They prepared electrospun Janus bilayers from polyvinyl chloride (PVC) and PCL, which mimicked Mimosa pudica opening and closing. They showed the possible design of complex microchannel fabrication and as well they were able to achieve high flow rates (4.7 μL s^{-1}) that are two orders of magnitude higher than traditional wicking-based

**ADVANCED
SCIENCE NEWS**
www.advancedsciencenews.com

**ADVANCED
FUNCTIONAL
MATERIALS**
www.afm-journal.de

devices. These both approaches show the future possibility to fully design microfluidic device from fast, responsive shape transforming soft materials.

4.1.3. Sensors

Fast response time, various stimuli, and macroscopic shape change are assets of shape transforming soft materials that make them attractive for sensor development. Shape transforming materials like hydrogels can respond to stimuli like temperature, pH, specific ions, and chemicals, which makes them suitable for sensing. Usually, atomic force microscope (AFM) cantilevers are used to make hydrogel-based sensors; one side of the cantilever is covered with hydrogel layer, and AFM cantilever bends accordingly to the swelling state of hydrogel.[135–137] The bending of the cantilever can be detected by a change in reflection of the laser beam of the cantilever surface. This kind of sensing method is simple and easy to use; any AFM device can be used for this method. Zhang et al. described more advance sensing by using stimuli-responsive hydrogel as a spacing transducer in-between nanodiamond and magnetic nanoparticles[138] (Figure 11e). The use of nanodiamond center-based magnetometry provides the ability to use the system for quantum biosensing, but unfortunately, they are unable to sense parameters like pressure and temperature and can be influenced by parameters like pH and nonmagnetic biomolecules. As a solution to these problems, they use hydrogel that fully covers nanodiamond, and then they docked magnetic nanoparticles on top of the hydrogel shell. Due to hydrogel swelling and shrinking, there is a sharp variation in the separation distance of diamond and nanoparticles, which makes a change in the magnetic field, and these changes can be detected easily by nanodiamond center. The hybrid sensor showed reversibility and stability for more than one week and higher sensibility then nanodiamond alone in the same conditions. With proper design and this hybrid system can be used for sensing other physiological parameters: pH, enzymes, sugar, and other types of nonmagnetic biomolecules.

4.1.4. Electronic Devices

Shape transforming soft materials can be used in electronic devices because of their ability to change the form as well generate the force as mentioned before. For example, Kim et al. have designed 3D printed soft materials that contain programmed ferromagnetic domains that were able to exhibit electric functions[139] (Figure 11f). These ferromagnetic domains were printed using composite ink of magnetizable particles, fumed silica particles, and rated silicone rubber matrix. During 3D printing, they applied a magnetic field to the dispensing nozzle to align the magnetic particle in ferromagnetic domains. When the magnetic field is applied to the printed substrate, it induces torques on the embedded ferromagnetic particles forming stresses that lead to macroscale material response. To test designed structure ability to be used as flexible electronics, they added components like PDMS insulator, conductive silver ink, magnetic ink, and two-color LEDs. By changing magnetic field direction, they were

able to switch on red or green LED, depending on magnetic particle arrangement in the ferromagnetic domain. This platform can be further examined with various elastomer and hydrogel matrices as well as the change of magnetic particles. Rodgers and their group have been working on various shape-transforming electronic devices.[140–142] Their latest research describes microelectronic devices that can be actuated by multistable buckling mechanics[140] (Figure 11g). Prepared mesostructures could be reconfigured in three to four different states, showing their versatility. To show the potential of using these shape transforming materials for electronic devices, they integrated silicon n-channel metal-oxide-semiconductor field-effect transistors (n-MOSFET) and μ-LEDs on top of 3D mesostructure. To show potential for wireless communication of these microelectronic devices, they used passive radiofrequency circuits and concealable antennas.

4.2. Shape Transformation Affect Material Properties

4.2.1. Smart Textiles

Smart textile is a promising application for shape memory polymers (SMPs). Smart textiles can be designed by using single actuating SMPs fibers that are incorporated in textiles; this single fiber actuates with the change of humidity and/or temperature, which leads to shrinking and folding of the whole textile. This concept has been shown by designer Leenders using a hairdryer and incorporating nitinol fiber inside of textile, with increase and decrease of the temperature sleeves of textile can be rolled up or down.[143]

As another option, we described the method of producing non-crosslinked shape-transforming Janus fibers for smart textile applications.[144] 3D printing and melt-spinning were used to obtain Janus fibers consisting of fusible PCL as first polymer and acrylonitrile butadiene styrene (ABS) or polylactide (PLA) as the second polymer. ABS and PLA were chosen as the second polymer because of their high softening point (Figure 11h). This Janus fiber model was able to show reversible actuation due to the contraction of PCL polymer in the presence of entanglements during crystallization and relaxation of stressed nonfusible side during melting. Design fibers demonstrate various advantages in comparison to existing smart fibers like fast actuation rate, reversible actuation, actuation temperature range from 0–70 °C, and high plasticity for repair when the fiber is deformed or broken.

4.2.2. Drug Delivery

The main challenge of drug delivery is to transfer the necessary concentration of drugs to the intended site of action. As high doses are necessary in most cases, there is a high risk of potential side effects and reduced efficiency when the drug is absorbed in various parts of the human body and cannot reach the intended site.[128,145–147] As a solution to this problem, scientists are working on multiple systems that could reach the intended site in a controlled manner and could release drugs based on specific environmental cues.[148] Shape transforming

**ADVANCED
SCIENCE NEWS**
www.advancedsciencenews.com

**ADVANCED
FUNCTIONAL
MATERIALS**
www.afm-journal.de

soft materials can be used for drug encapsulation and can be controlled by adding on removing stimuli, thus being a good model for targeted drug delivery. Nevertheless, drug release depends on the surface to volume ratio, which makes changes of the surface to volume ratio during swelling of stimuli-responsive material especially interesting for drug delivery.[7,149] Gracias and his group have designed stimuli-responsive theragrippers for chemomechanical-controlled release of fluorescent dyes and commercial drugs like mesalamine and doxorubicin[150] (Figure 11i). They used photolithography to design theragrippers that consisted of rigid poly(propylene fumarate) segments and stimuli-responsive poly(N-isopropylacrylamide-co-acrylic acid) hinges. Due to thermos-responsive hinges, gripper closes above 32 °C temperature allowing it to grip onto tissue when it reaches body temperature from a cold state. Theragrippers showed improved site-specific delivery and time-tunable drug release, making it suitable for applicability in the gastrointestinal tract.

4.2.3. Optical Devices

Microlenses with tunable focal length can be designed using stimuli-responsive hydrogels. In this case, focal length depends on particle size, which changes with the swelling degree of hydrogel after external stimuli are added to the system.[29,151,152] Another approach describes water–oil interface liquid microlenses that are mounted on a ring formed by macroscopic stimuli-responsive hydrogel [153](Figure 11j). When appropriate stimuli were added to the system, the hydrogel ring underneath the aperture expanded or shrunk. The actuation of hydrogel induces volume change of water droplet in the middle of the ring. Variations of the volume enclosed by the ring and volume of the water droplet generate pressure difference across the water–oil interface that regulates the geometry of the liquid meniscus. These lenses showed a fast response rate and did not require a complicated external control system.

4.3. Shape Generation During Transformation

4.3.1. Tissue Engineering

While the world's populations are increasing and aging, scientists have focused on tissue engineering field to solve the challenge of organ and tissue shortage and provide a new treatment for patients.[7,128,154] Using tissue-engineering techniques, we can replace, preserve and regenerate different tissues and organs.[128,154,155] Material ability to transform its shape is promising for the field of tissue engineering; because of dynamic shape change, we would be able to achieve less invasive surgical procedures.[156] Shape-transforming soft materials can be used for various tissue regeneration as cardiac, bone, skeletal, vascular and endothelial.[7,157]

An important feature for shape transformation soft materials is their easy and reversible transformation from flat 2D sheet to the 3D tubular structure. This approach is crucial for tubular human tissue formation like skeletal muscle bundles, ves-sels, and arteries, osteons, axons, etc. For example, Zhao et al. described shape morphing scaffolds for 3D endothelialization, where they co-electrospun functional polycaprolactone (PCL) and methacrylated gelatin (GelMA) layer on top of biocompatible shaping SMPs film for better cell adhesion[158] (Figure 11k). Endothelial cells showed high seeding efficiency and cell viability on shape morphing constructs that were able to perform shape transformation in physiological temperature. These tubular structures showed potential for small diameter vascular graft formation with improved endothelialization. Similarly Vannozzi et al.[159] (Figure 11l), showed the potential of using poly(ethylene glycol) diacrylate (PEGDA) bilayers for implantable fascicle-like muscle cell fabrication. Two different molecular weight PEGDA was used to achieve and control folding behavior, based on each layer thickness. Cardiac and muscle cells exhibited high cell viability and preserved their contractile function. As well, electrospun bilayers with no supportive layer had showed potential to be used in tissue engineering for cell encapsulation. Apsite et al. designed multilayer electrospun mesh system consisting of PCL and PNIPAM, that can self-fold in physiological conditions and sustain cell viability[160] (Figure 11m).

4.3.2. Shape-Transforming Origami

Term Origami is used to describe folding paper art coming from Japan, where a 2D flat sheet is folded in various complex 3D structures like crane, rhino, and various other animals. Following simple axioms and theorems it is possible to fold any soft or rigid material, which makes this principle more attractive to industrial applications as solar panels, space telescopes, stents for medical purposes, high tech origami, grocery bags, vacuumatics, programmable matter folding.[161] Shape transforming has been widely used for development of foldable devices. R. Wood and his group have developed wireless multijoint folding robots based on shape memory polymer origami-based foldable robot that was able to self-fold, actuate and even degrade in acetone or water.[162] Origami robot was thermally activated and due to cubic neodymium magnet that was incorporated in polystyrene robot, they were able to control direction of locomotion using magnetic field. These kinds of origami-based complex 3D structures can be in future used in vivo. In most recent research, they prepared device that was based on electromagnetic power transmission and resonance selectivity[163] (Figure 11n). They achieve folding using magnetically active shape memory alloy (SMA) actuator as the electrical load, which does not require any physical contact and allows to actuate each SMA individually or in groups. The advantage of this method is that you can prepare robotic systems small weight like 0.8 g and still have high energy density.

5. Summary and Outlook

There is considerable progress in the development of materials with shape-changing properties as well as in understanding and programming of shape transformation that allows a broad variety in shapes. The controlled shape transformation can be

utilized for diverse applications including soft robotics, micro-fluidics, sensory, electronic devices, smart textiles, drug delivery, optical devices, tissue engineering. In spite of significant prepared progress in all these areas, properties of available materials are not always optimal from point of view of particular applications. For example, shape transformation requires high mobility of polymer chains and is observed above melting/glass transition point. Moreover, reversibility of actuation requires crosslinking of polymers. In other words, polymers have properties of elastomer in the state when they actuate. Elastic modulus of elastomer depends on crosslinking density and typically is in the order of megapascals. Crosslinking density is even lower in swollen elastomers (gels), and therefore, they are even softer. The force generated during the actuation of shape-changing polymers is roughly elastic modulus multiplied by actuation amplitude. This force is usually much lower than the force generated by hard motors/actuators. Therefore, shape-changing polymers are unable to compete with classic motor-based actuators in conventional robotics. On the other hand, due to their softness, shape-changing polymers have distinct advantages in the "soft" applications such as soft robotics, tissue engineering, flexible optics, where "hard" actuators cannot be applied. Moreover, due to their softness, shape-changing polymers allow considerable amplitude of shape transformation at lower absorbed energy. Although basic principles of application of shape-changing polymers in these fields have been successfully demonstrated, their practical application is still problematic because each of these "soft" applications put new requirements for properties of materials. For example, optical devices may require either high transparency of polymers or their special optical properties. Bio-related applications like tissue engineering and drug delivery require biocompatible and biodegradable shape-changing polymers, which are also able to change their shape at the conditions acceptable for living matter. Thus, the first open problem is the precise tailoring of the properties of shape-changing polymers.

The second problem is the weakness of the materials. Shape transformation is often accompanied by considerable local deformations, which may lead to rupture of materials. Therefore, the development of self-healing shape-changing materials can be one of the future directions of development. Although the task may look simple because there are many approaches for the design of self-healing materials, the real solution for this problem is difficult. In fact, the self-healing of cracks is commonly based on the interdiffusion of chain segments and the reversibility of bonds. Both these processes assume plastic deformation of materials, i.e., actuator will undergo not pure elastic but visco-elastic deformation and reversibility of actuation will not be complete.

The third big challenge in the field of microfabrication using controlled shape transformation is miniaturization. Fabrication of micrometer—size shape-changing structures is a multistep procedure, which is very expensive and requires the use of sophisticated equipment. Recently, 3D printing became very popular for fabrication shape-changing structures that have even led to the development of the new area in 3D printing–4D printing. There are several most widely used 3D printing techniques, but no one of them allows the fabrication of microstructures at low costs. Indeed, fused deposition modeling (FDM) printing allows fabrication of multicomponent structures, but its resolution is ca 100–200 µm. Stereolithography allows a much better resolution, which is ca 10 µm, it can hardly be used for fabrication of multicomponent objects as it requires a constant exchange of photopolymer. Ink-jet printing and similar drop-based technologies allow high resolution but operate with low viscosity liquids such as oligomer/monomer solution, which have to be photopolymerized afterward. Melt electrospinning writing is a very interesting method for the fabrication of very fine structures from viscous polymer melts. This method is however based on the deposition of continuous fibers and fabrication of dots and discrete elements not possible. All this means that currently a combination of different 3D printing methods is needed for microfabrication of shape-changing structures.

Forth challenge related to microfabrication is the precise programming of shape transformation. There are brilliant works[164,165] demonstrating impressive possibilities to program the folding, there are still unsolved problems related to stability, reversibility, and possibilities to reprogram the folding. For example, there is no report about a shape-changing material which allows full flexibility of folding when (i) the same film can be folded and unfolded in a variety of ways and (ii) there is a possibility to decide if folding is reversible or irreversible, that must allow fixation of folded structures. The reason for these effects is the intrinsic properties of individual shape-changing materials. As an illustration, the hydrogel-based shape-changing film can fold in various ways depending on their structure. On the other hand, as soon as stimuli are removed the shape of folded objects changes. The same happens when the hydrogel layer dries.

In summary, the microfabrication using shape-changing polymers is a rapidly developing field, and many new excellent works are published on this topic each day. Despite this, there are still many problems to be solved before microfabrication using shape-changing polymers became real technology.

Acknowledgements

Conflict of Interest

The authors declare no conflict of interest.

Keywords

[1] S. Ford, T. Minshall, *Addit. Manuf.* **2019**, *25*, 131.
[2] T. D. Ngo, A. Kashani, G. Imbalzano, K. T. Q. Nguyen, D. Hui, *Composites, Part B* **2018**, *143*, 172.
[3] Y. Zhou, *J. Biomed. Sci.* **2017**, *24*, 80.

**ADVANCED
Science News**

www.advancedsciencenews.com

**ADVANCED
FUNCTIONAL
MATERIALS**

www.afm-journal.de

[4] A. Lendlein, S. Kelch, *Angew. Chem., Int. Ed.* **2002**, *41*, 2034.

[5] Q. Zhao, M. Behl, A. Lendlein, *Soft Matter* **2013**, *9*, 1744.

[6] M. Behl, J. Zotzmann, A. Lendlein, *Adv. Polym. Sci.* **2010**, *226*, 1.

[7] A. Kirillova, L. Ionov, *J. Mater. Chem. B* **2019**, *7*, 1597.

[8] Q. Zhao, H. J. Qi, T. Xie, *Prog. Polym. Sci.* **2015**, *49–50*, 79.

[9] A. Biswas, A. P. Singh, D. Rana, V. K. Aswal, P. Maiti, *Nanoscale* **2018**, *10*, 9917.

[10] J. Dong, R. A. Weiss, *Macromolecules* **2011**, *44*, 8871.

[11] R. Dolog, R. A. Weiss, *Macromolecules* **2013**, *46*, 7845.

[12] A. Biswas, V. K. Aswal, P. Maiti, *J. Colloid Interface Sci.* **2019**, *556*, 147.

[13] H. Tobushi, N. Ito, K. Takata, S. Hayashi, *Mater. Sci. Forum* **2000**, *327–328*, 343.

[14] H. Tobushi, T. Hashimoto, S. Hayashi, E. Yamada, *J. Intell. Mater. Syst. Struct.* **1997**, *8*, 711.

[15] T. D. Nguyen, H. J. Qi, F. Castro, K. N. Long, *J. Mech. Phys. Solids* **2008**, *56*, 2792.

[16] A. D. Mulliken, M. C. Boyce, *Int. J. Solids Struct.* **2006**, *43*, 1331.

[17] J. Zhou, Q. X. Li, S. A. Turner, V. S. Ashby, S. S. Sheiko, *Polymer* **2015**, *72*, 464.

[18] C. A. Avila-Orta, F. J. Medellin-Rodriguez, Z. G. Wang, D. Navarro-Rodriguez, B. S. Hsiao, F. J. Yeh, *Polymer* **2003**, *44*, 1527.

[19] M. Behl, K. Kratz, U. Noechel, T. Sauter, A. Lendlein, *Proc. Natl. Acad. Sci. USA* **2013**, *110*, 12555.

[20] A. Biswas, V. K. Aswal, P. U. Sastry, D. Rana, P. Maiti, *Macromolecules* **2016**, *49*, 4889.

[21] R. Pelrine, R. Kornbluh, Q. B. Pei, J. Joseph, *Science* **2000**, *287*, 836.

[22] F. Carpi, D. De Rossi, *Mater. Sci. Eng., C* **2004**, *24*, 555.

[23] F. Carpi, C. Salaris, D. De Rossi, *Smart Mater. Struct.* **2007**, *16*, S300.

[24] S. Shian, K. Bertoldi, D. R. Clarke, *Adv. Mater.* **2015**, *27*, 6814.

[25] S. Shian, R. M. Diebold, D. R. Clarke, *Opt. Express* **2013**, *21*, 8669.

[26] E. Hajiesmaili, D. R. Clarke, *Nat. Commun.* **2019**, *10*, 183.

[27] Y. Osada, A. Matsuda, *Nature* **1995**, *376*, 219.

[28] C. C. Wang, W. M. Huang, Z. Ding, Y. Zhao, H. Purnawali, *Compos. Sci. Technol.* **2012**, *72*, 1178.

[29] L. Ionov, *Mater. Today* **2014**, *17*, 494.

[30] K. Inomata, T. Terahama, R. Sekoguchi, T. Ito, H. Sugimoto, E. Nakanishi, *Polymer* **2012**, *53*, 3281.

[31] A. Yasin, H. Z. Li, Z. Lu, S. U. Rehman, M. Siddiq, H. Y. Yang, *Soft Matter* **2014**, *10*, 972.

[32] R. D. Harris, J. T. Auletta, S. A. M. Motlagh, M. J. Lawless, N. M. Perri, S. Saxena, L. M. Weiland, D. H. Waldeck, W. W. Clark, T. Y. Meyer, *ACS Macro Lett.* **2013**, *2*, 1095.

[33] X.-J. Han, Z.-Q. Dong, M.-M. Fan, Y. Liu, J.-H. li, Y.-F. Wang, Q.-J. Yuan, B.-J. Li, S. Zhang, *Macromol. Rapid Commun.* **2012**, *33*, 1055.

[34] O. Peters, H. Ritter, *Angew. Chem., Int. Ed.* **2013**, *52*, 8961.

[35] Z.-Q. Dong, Y. Cao, Q.-J. Yuan, Y.-F. Wang, J.-H. Li, B.-J. Li, S. Zhang, *Macromol. Rapid Commun.* **2013**, *34*, 867.

[36] T. Miyata, N. Asami, T. Uragami, *Nature* **1999**, *399*, 766.

[37] H. R. Brand, H. Pleiner, P. Martinoty, *Soft Matter* **2006**, *2*, 182.

[38] X. J. Wang, *Prog. Polym. Sci.* **1997**, *22*, 735.

[39] D. L. Thomsen, P. Keller, J. Naciri, R. Pink, H. Jeon, D. Shenoy, B. R. Ratna, *Macromolecules* **2001**, *34*, 5868.

[40] I. Kundler, H. Finkelmann, *Macromol. Chem. Phys.* **1998**, *199*, 677.

[41] J. Naciri, A. Srinivasan, H. Jeon, N. Nikolov, P. Keller, B. R. Ratna, *Macromolecules* **2003**, *36*, 8499.

[42] E. M. Terentjev, M. Warner, G. C. Verwey, *J. Phys. II* **1996**, *6*, 1049.

[43] P.-G. De Gennes, M. Hébert, R. Kant, *Macromol. Symp.* **1997**, *113*, 39.

[44] Z. Pei, Y. Yang, Q. Chen, E. M. Terentjev, Y. Wei, Y. Ji, *Nat. Mater.* **2014**, *13*, 36.

[45] T. Ikeda, M. Nakano, Y. Yu, O. Tsutsumi, A. Kanazawa, *Adv. Mater.* **2003**, *15*, 201.

[46] M.-H. Li, P. Keller, B. Li, X. Wang, M. Brunet, *Adv. Mater.* **2003**, *15*, 569.

[47] Y. Yang, W. Zhan, R. Peng, C. He, X. Pang, D. Shi, T. Jiang, Z. Lin, *Adv. Mater.* **2015**, *27*, 6376.

[48] C. Ohm, M. Brehmer, R. Zentel, *Adv. Mater.* **2010**, *22*, 3366.

[49] Y. L. Yu, T. Ikeda, *Angew. Chem., Int. Ed.* **2006**, *45*, 5416.

[50] M. Behl, K. Kratz, J. Zotzmann, U. Nöchel, A. Lendlein, *Adv. Mater.* **2013**, *25*, 4466.

[51] F. Zou, S. Chen, *Mater. Today: Proc.* **2019**, *16*, 1548.

[52] M. Boncheva, D. A. Bruzewicz, G. M. Whitesides, *Pure Appl. Chem.* **2003**, *75*, 621.

[53] N. Chakrapani, B. Wei, A. Carrillo, P. M. Ajayan, R. S. Kane, *Proc. Natl. Acad. Sci. USA* **2004**, *101*, 4009.

[54] N. Bowden, I. S. Choi, B. A. Grzybowski, G. M. Whitesides, *J. Am. Chem. Soc.* **1999**, *121*, 5373.

[55] R. Pericet-Cámara, A. Best, H.-J. Butt, E. Bonaccurso, *Langmuir* **2008**, *24*, 10565.

[56] A. I. Rusanov, *J. Colloid Interface Sci.* **1978**, *63*, 330.

[57] G. R. Lester, *J. Colloid Sci.* **1961**, *16*, 315.

[58] B. Roman, J. Bico, *J. Phys.: Condens. Matter.* **2010**, *22*, 493101.

[59] X. Guo, H. Li, B. Yeop Ahn, E. B. Duoss, K. J. Hsia, J. A. Lewis, R. G. Nuzzo, *Proc. Natl. Acad. Sci. USA* **2009**, *106*, 20149.

[60] X. Xu, A. Jagota, S. Peng, D. Luo, M. Wu, C.-Y. Hui, *Langmuir* **2013**, *29*, 8665.

[61] Y. Zhang, Y. Li, W. Liu, *Adv. Funct. Mater.* **2015**, *25*, 471.

[62] M. Balk, M. Behl, A. Lendlein, *Smart Mater. Struct.* **2019**, *28*, 055026.

[63] Y. C. Zhang, J. X. Liao, T. Wang, W. X. Sun, Z. Tong, *Adv. Funct. Mater.* **2018**, *28*, 1707245.

[64] J. Odent, T. J. Wallin, W. Pan, K. Kruemplestaedter, R. F. Shepherd, E. P. Giannelis, *Adv. Funct. Mater.* **2017**, *27*, 1701807.

[65] H. Guo, C. Mussault, A. Marcellan, D. Hourdet, N. Sanson, *Macromol. Rapid Commun.* **2017**, *38*, 1700287.

[66] R. Luo, J. Wu, N.-D. Dinh, C.-H. Chen, *Biomicrofluidics* **2015**, *25*, 7272.

[67] Y. Yang, Y. Tan, X. Wang, W. An, S. Xu, W. Liao, Y. Wang, *ACS Appl. Mater. Interfaces* **2018**, *10*, 7688.

[68] T. Wang, J. Huang, Y. Yang, E. Zhang, W. Sun, Z. Tong, *ACS Appl. Mater. Interfaces* **2015**, *7*, 23423.

[69] Y. Zhou, J. Tan, D. Chong, X. Wan, J. Zhang, *Adv. Funct. Mater.* **2019**, *29*, 1901202.

[70] N. Van Herck, F. E. Du Prez, *Macromolecules* **2018**, *51*, 3405.

[71] A. Melocchi, N. Inverardi, M. Uboldi, F. Baldi, A. Maroni, S. Pandini, F. Briatico-Vangosa, L. Zema, A. Gazzaniga, *Int. J. Pharm.* **2019**, *559*, 299.

[72] T. Chatterjee, P. Dey, G. B. Nando, K. Naskar, *Polymer* **2015**, *78*, 180.

[73] K. J. Wang, X. X. Zhu, *ACS Biomater. Sci. Eng.* **2018**, *4*, 3099.

[74] Y. T. Yao, T. Y. Zhou, J. J. Wang, Z. H. Li, H. B. Lu, Y. J. Liu, J. S. Leng, *Composites, Part A* **2016**, *90*, 502.

[75] J. Zotzmann, M. Behl, D. Hofmann, A. Lendlein, *Adv. Mater.* **2010**, *22*, 3424.

[76] R. Pelrine, R. Kornbluh, Q. Pei, J. Joseph, *Science* **2000**, *287*, 836.

[77] F. Carpi, D. De Rossi, *Mater. Sci. Eng., C* **2004**, *24*, 555.

[78] F. Carpi, C. Salaris, D. D. Rossi, *Smart Mater. Struct.* **2007**, *16*, S300.

[79] H. Imamura, K. Kadooka, M. Taya, *Soft Matter* **2017**, *13*, 3440.

[80] T.-G. La, G.-K. Lau, L.-L. Shiau, A. W. Y. Tan, *Proc. SPIE* **2014**, *9056*, 90560X.

[81] D. J. Roach, C. Yuan, X. Kuang, V. C. F. Li, P. Blake, M. L. Romero, I. Hammel, K. Yu, H. J. Qi, *ACS Appl. Mater. Interfaces* **2019**, *11*, 19514.

[82] A. Kotikian, R. L. Truby, J. W. Boley, T. J. White, J. A. Lewis, *Adv. Mater.* **2018**, *30*, 1706164.

[83] L. Yu, H. Shahsavan, G. Rivers, C. Zhang, P. X. Si, B. X. Zhao, *Adv. Funct. Mater.* **2018**, *28*, 1802809.

[84] B. T. Michal, B. M. McKenzie, S. E. Felder, S. J. Rowan, *Macromolecules* **2015**, *48*, 3239.

[85] W. Wu, L. M. Yao, T. S. Yang, R. Y. Yin, F. Y. Li, Y. L. Yu, *J. Am. Chem. Soc.* **2011**, *133*, 15810.

[86] L. Liu, M.-H. Liu, L.-L. Deng, B.-P. Lin, H. Yang, *J. Am. Chem. Soc.* **2017**, *139*, 11333.

[87] L. Ionov, *Macromol. Chem. Phys.* **2013**, *214*, 1178.

[88] E. D. Demaine, *Discrete and Computational Geometry*, Springer, Heidelberg **2001**.

[89] C. Lauff, T. W. Simpson, M. Frecker, Z. Ounaies, S. Ahmed, P. von Lockette, R. Strzelec, R. Sheridan, J.-M. Lien, presented at ASME 2014 Int. Design Engineering Technical Conf. and Computers and Information in Engineering Conf., Buffalo, NY, August **2014**.

[90] J. Ryu, M. D'Amato, X. Cui, K. N. Long, H. J. Qi, M. L. Dunn, *Appl. Phys. Lett.* **2012**, *100*, 161908.

[91] Q. Ge, C. K. Dunn, H. J. Qi, M. L. Dunn, *Smart Mater. Struct.* **2014**, *23*, 094007.

[92] L. Ionov, *Polym. Rev.* **2013**, *53*, 92.

[93] J. T. Wu, C. Yuan, Z. Ding, M. Isakov, Y. Q. Mao, T. J. Wang, M. L. Dunn, H. J. Qi, *Sci. Rep.* **2016**, *6*, 24224.

[94] S. Tibbits, *Archit. Des.* **2014**, *84*, 116.

[95] A. S. Gladman, E. A. Matsumoto, R. G. Nuzzo, L. Mahadevan, J. A. Lewis, *Nat. Mater.* **2016**, *15*, 413.

[96] Q. Zhang, K. Zhang, G. Hu, *Sci. Rep.* **2016**, *6*, 22431.

[97] J. Ryu, M. D'Amato, X. D. Cui, K. N. Long, H. J. Qi, M. L. Dunn, *Appl. Phys. Lett.* **2012**, *100*, 161908.

[98] S. Armon, H. Aharoni, M. Moshe, E. Sharon, *Soft Matter* **2014**, *10*, 2733.

[99] S. Janbaz, R. Hedayati, A. A. Zadpoor, *Mater. Horiz.* **2016**, *3*, 536.

[100] T. van Manen, S. Janbaz, A. A. Zadpoor, *Mater. Today* **2018**, *21*, 144.

[101] Z. Zhao, J. Wu, X. Mu, H. Chen, H. J. Qi, D. Fang, *Sci. Adv.* **2017**, *3*, e1602326.

[102] G. F. Hu, A. R. Damanpack, M. Bodaghi, W. H. Liao, *Smart Mater. Struct.* **2017**, *26*, 125023.

[103] P. Cendula, S. Kiravittaya, Y. F. Mei, C. Deneke, O. G. Schmidt, *Phys. Rev. B* **2009**, *79*, 085429.

[104] R. Mohr, K. Kratz, T. Weigel, M. Lucka-Gabor, M. Moneke, A. Lendlein, *Proc. Natl. Acad. Sci. USA* **2006**, *103*, 3540.

[105] H. Y. Jiang, S. Kelch, A. Lendlein, *Adv. Mater.* **2006**, *18*, 1471.

[106] Y. Liu, J. K. Boyles, J. Genzer, M. D. Dickey, *Soft Matter* **2012**, *8*, 1764.

[107] A. M. Schmidt, *Macromol. Rapid Commun.* **2006**, *27*, 1168.

[108] Y. Liu, B. Shaw, M. D. Dickey, J. Genzer, *Sci. Adv.* **2017**, *3*, e1602417.

[109] D. Habault, H. Zhang, Y. Zhao, *Chem. Soc. Rev.* **2013**, *42*, 7244.

[110] Q. Shen, S. Trabia, T. Stalbaum, V. Palmre, K. Kim, I.-K. Oh, *Sci. Rep.* **2016**, *6*, 24462.

[111] M. T. Tolley, S. M. Felton, S. Miyashita, D. Aukes, D. Rus, R. J. Wood, *Smart Mater. Struct.* **2014**, *23*, 094006.

[112] B. Jin, H. Song, R. Jiang, J. Song, Q. Zhao, T. Xie, *Sci. Adv.* **2018**, *4*, eaao3865.

[113] T. G. Leong, A. M. Zarafshar, D. H. Gracias, *Small* **2010**, *6*, 792.

[114] N. Bassik, B. T. Abebe, K. E. Laflin, D. H. Gracias, *Polymer* **2010**, *51*, 6093.

[115] J. Kim, J. A. Hanna, M. Byun, C. D. Santangelo, R. C. Hayward, *Science* **2012**, *335*, 1201.

[116] J.-H. Na, A. A. Evans, J. Bae, M. C. Chiappelli, C. D. Santangelo, R. J. Lang, T. C. Hull, R. C. Hayward, *Adv. Mater.* **2015**, *27*, 79.

[117] G. Stoychev, S. Turcaud, J. W. C. Dunlop, L. Ionov, *Adv. Funct. Mater.* **2013**, *23*, 2295.

[118] R. M. Erb, J. S. Sander, R. Grisch, A. R. Studart, *Nat. Commun.* **2013**, *4*, 1712.

[119] C. L. van Oosten, C. W. M. Bastiaansen, D. J. Broer, *Nat. Mater.* **2009**, *8*, 677.

[120] M. Camacho-Lopez, H. Finkelmann, P. Palffy-Muhoray, M. Shelley, *Nat. Mater.* **2004**, *3*, 307.

[121] L. T. de Haan, C. Sánchez-Somolinos, C. M. W. Bastiaansen, A. P. H. J. Schenning, D. J. Broer, *Angew. Chem., Int. Ed.* **2012**, *51*, 12469.

[122] Y. Sawa, F. Ye, K. Urayama, T. Takigawa, V. Gimenez-Pinto, R. L. B. Selinger, J. V. Selinger, *Proc. Natl. Acad. Sci. USA* **2011**, *108*, 6364.

[123] K. M. Lee, T. J. Bunning, T. J. White, *Adv. Mater.* **2012**, *24*, 2839.

[124] L. T. de Haan, V. Gimenez-Pinto, A. Konya, T.-S. Nguyen, J. M. N. Verjans, C. Sánchez-Somolinos, J. V. Selinger, R. L. B. Selinger, D. J. Broer, A. P. H. J. Schenning, *Adv. Funct. Mater.* **2014**, *24*, 1251.

[125] X. Lu, S. Guo, X. Tong, H. Xia, Y. Zhao, *Adv. Mater.* **2017**, *29*, 1606467.

[126] S. Palagi, A. G. Mark, S. Y. Reigh, K. Melde, T. Qiu, H. Zeng, C. Parmeggiani, D. Martella, A. Sanchez-Castillo, N. Kapernaum, F. Giesselmann, D. S. Wiersma, E. Lauga, P. Fischer, *Nat. Mater.* **2016**, *15*, 647.

[127] G. Stoychev, A. Kirillova, L. Ionov, *Adv. Opt. Mater.* **2019**, *7*, 1900067.

[128] O. Erol, A. Pantula, W. Liu, D. H. Gracias, *Adv. Mater. Technol.* **2019**, *4*, 1900043.

[129] H. Cui, Q. Zhao, Y. Wang, X. Du, *Chem. - Asian J.* **2019**, *14*, 2369.

[130] D. Han, C. Farino, C. Yang, T. Scott, D. Browe, W. Choi, J. W. Freeman, H. Lee, *ACS Appl. Mater. Interfaces* **2018**, *10*, 17512.

[131] C. Huang, J.-a. Lv, X. Tian, Y. Wang, Y. Yu, J. Liu, *Sci. Rep.* **2015**, *5*, 17414.

[132] G. M. Whitesides, *Nature* **2006**, *442*, 368.

[133] L. D'Eramo, B. Chollet, M. Leman, E. Martwong, M. Li, H. Geisler, J. Dupire, M. Kerdraon, C. Vergne, F. Monti, P. Tran, P. Tabeling, *Microsyst. Nanoeng.* **2018**, *4*, 17069.

[134] W. S. Y. Wong, M. Li, D. R. Nisbet, V. S. J. Craig, Z. Wang, A. Tricoli, *Sci. Adv.* **2016**, *2*, e1600417.

[135] L. Ionov, *Langmuir* **2015**, *31*, 5015.

[136] R. Bashir, J. Z. Hilt, O. Elibol, A. Gupta, N. A. Peppas, *Appl. Phys. Lett.* **2002**, *81*, 3091.

[137] J. Z. Hilt, A. K. Gupta, R. Bashir, N. A. Peppas, *Biomed. Microdevices* **2003**, *5*, 177.

[138] T. Zhang, G.-Q. Liu, W.-H. Leong, C.-F. Liu, M.-H. Kwok, T. Ngai, R.-B. Liu, Q. Li, *Nat. Commun.* **2018**, *9*, 3188.

[139] Y. Kim, H. Yuk, R. Zhao, S. A. Chester, X. Zhao, *Nature* **2018**, *558*, 274.

[140] H. Fu, K. Nan, W. Bai, W. Huang, K. Bai, L. Lu, C. Zhou, Y. Liu, F. Liu, J. Wang, M. Han, Z. Yan, H. Luan, Y. Zhang, Y. Zhang, J. Zhao, X. Cheng, M. Li, J. W. Lee, Y. Liu, D. Fang, X. Li, Y. Huang, Y. Zhang, J. A. Rogers, *Nat. Mater.* **2018**, *17*, 268.

[141] Z. Yan, M. Han, Y. Shi, A. Badea, Y. Yang, A. Kulkarni, E. Hanson, M. E. Kandel, X. Wen, F. Zhang, Y. Luo, Q. Lin, H. Zhang, X. Guo, Y. Huang, K. Nan, S. Jia, A. W. Oraham, M. B. Mevis, J. Lim, X. Guo, M. Gao, W. Ryu, K. J. Yu, B. G. Nicolau, A. Petronico, S. S. Rubakhin, J. Lou, P. M. Ajayan, K. Thornton, G. Popescu, D. Fang, J. V. Sweedler, P. V. Braun, H. Zhang, R. G. Nuzzo, Y. Huang, Y. Zhang, J. A. Rogers, *Proc. Natl. Acad. Sci. USA* **2017**, *114*, E9455.

[142] C. Yu, Z. Duan, P. Yuan, Y. Li, Y. Su, X. Zhang, Y. Pan, L. L. Dai, R. G. Nuzzo, Y. Huang, H. Jiang, J. A. Rogers, *Adv. Mater.* **2013**, *25*, 1541.

[143] M. Leenders, Shape Memory Textile Jacket, https://www.youtube.com/watch?v=EikQOrLyc-A (accessed: December 2019).

[144] L. Ionov, G. Stoychev, D. Jehnichen, J. U. Sommer, *ACS Appl. Mater. Interfaces* **2017**, *9*, 4873.

[145] S. Mitragotri, P. A. Burke, R. Langer, *Nat. Rev. Drug Discovery* **2014**, *13*, 655.

[146] A. S. Hoffman, *J. Controlled Release* **2008**, *132*, 153.

[147] J. Li, D. J. Mooney, *Nat. Rev. Mater.* **2016**, *1*, 16071.

[148] S. Fusco, M. S. Sakar, S. Kennedy, C. Peters, R. Bottani, F. Starsich, A. Mao, G. A. Sotiriou, S. Pané, S. E. Pratsinis, D. Mooney, B. J. Nelson, *Adv. Mater.* **2014**, *26*, 952.

[149] Y. Wang, Y. Miao, J. Zhang, J. P. Wu, T. B. Kirk, J. Xu, D. Ma, W. Xue, *Mater. Sci. Eng., C* **2018**, *84*, 44.

[150] K. Malachowski, J. Breger, H. R. Kwag, M. O. Wang, J. P. Fisher, F. M. Selaru, D. H. Gracias, *Angew. Chem., Int. Ed.* **2014**, *53*, 8045.

[151] J. Kim, M. J. Serpe, L. A. Lyon, *J. Am. Chem. Soc.* **2004**, *126*, 9512.

[152] J. Kim, N. Singh, L. A. Lyon, *Angew. Chem., Int. Ed.* **2006**, *45*, 1446.

[153] L. Dong, A. K. Agarwal, D. J. Beebe, H. Jiang, *Nature* **2006**, *442*, 551.

[154] J. L. Drury, D. J. Mooney, *Biomaterials* **2003**, *24*, 4337.

[155] L. E. Niklason, J. Gao, W. M. Abbott, K. K. Hirschi, S. Houser, R. Marini, R. Langer, *Science* **1999**, *284*, 489.

[156] S. Miao, H. Cui, M. Nowicki, S.-J. Lee, J. Almeida, X. Zhou, W. Zhu, X. Yao, F. Masood, M. W. Plesniak, M. Mohiuddin, L. G. Zhang, *Biofabrication* **2018**, *10*, 035007.

[157] L. Ionov, *Adv. Healthcare Mater.* **2018**, *7*, 1800412.

[158] Q. Zhao, J. Wang, H. Cui, H. Chen, Y. Wang, X. Du, *Adv. Funct. Mater.* **2018**, *28*, 1801027.

[159] L. Vannozzi, I. C. Yasa, H. Ceylan, A. Menciassi, L. Ricotti, M. Sitti, *Macromol. Biosci.* **2018**, *18*, 1700377.

[160] I. Apsite, G. Stoychev, W. Zhang, D. Jehnichen, J. Xie, L. Ionov, *Biomacromolecules* **2017**, *18*, 3178.

[161] L. J. Fei, D. Sujan, *Conf. Proc. IEEE Eng. Med. Biol. Soc.* **2013**, *7*, 229.

[162] S. Miyashita, S. Guitron, M. Ludersdorfer, C. R. Sung, D. Rus, *IEEE Int. Conf. on Robotics and Automation (ICRA)*, IEEE, Piscataway, NJ **2015**, pp. 1490–1496.

[163] M. Boyvat, J.-S. Koh, R. J. Wood, *Sci. Rob.* **2017**, *2*, eaan1544.

[164] J. L. Silverberg, J.-H. Na, A. A. Evans, B. Liu, T. C. Hull, C. D. Santangelo, R. J. Lang, R. C. Hayward, I. Cohen, *Nat. Mater.* **2015**, *14*, 389.

[165] J. L. Silverberg, A. A. Evans, L. McLeod, R. C. Hayward, T. Hull, C. D. Santangelo, I. Cohen, *Science* **2014**, *345*, 647.